ISOTOPIC INVESTIGATION OF ANTHROPOGENIC SOURCES OF ATMOSPHERIC NITROGEN AND CARBON ALONG SPATIAL GRADIENTS

by

Katherine Marie Middlecamp

Bachelor of Arts, University of Pittsburgh, 2005

Submitted to the Graduate Faculty of

College of Arts and Sciences in partial fulfillment

of the requirements for the degree of

Master of Arts in Geology & Planetary Science

University of Pittsburgh

2010

UNIVERSITY OF PITTSBURGH

COLLEGE OF ARTS AND SCIENCES

This thesis was presented

by

Katherine Marie Middlecamp

It was defended on

September 24, 2010

and approved by

Emily Elliott, PhD, Assistant Professor

Daniel Bain, PhD, Assistant Professor

Michael Rosenmeier, PhD, Assistant Professor

Thesis Director: Emily Elliott, PhD, Assistant Professor

ISOTOPIC INVESTIGATION OF ANTHROPOGENIC SOURCES OF ATMOSPHERIC NITROGEN AND CARBON ALONG SPATIAL GRADIENTS

Katherine Middlecamp, M.S.

University of Pittsburgh, 2010

Fossil fuel combustion from point and mobile sources is a key contributor to atmospheric CO_2, a major greenhouse gas, and NO_x, a precursor to acid rain and smog. Increased concentrations of these pollutants are found near the sources, i.e., in urban areas and close to roadways. Vegetation in urban and near-road environments represents an important sink for anthropogenic inputs of NO_x and CO_2, and understanding the nutrient dynamics of vegetation in urban and near-road ecosystems is critical to understanding budgets of NO_x and CO_2. However, little is known about how these ecosystems compensate for higher local atmospheric CO_2 and NO_x concentrations. This study uses stable isotope geochemistry to trace atmospheric nutrients to urban and roadway vegetation.

Chapter 1 presents an introduction to the environmental problems associated with atmospheric reactive nitrogen and CO_2, the use of stable isotopes to determine the sources of these pollutants, and a review of recent studies which use stable isotopes to determine the sources of plant nutrient uptake.

The study described in Chapter 2 examines the fate and transport of gaseous reactive nitrogen from mobile sources along a highway road gradient. This study uses stable isotopes of nitrogen in dry nitrogen deposition to examine the extent of nitrogen loading along a gradient perpendicular to a major highway. In addition, this study examines the effects of increased

roadway N deposition on local vegetation by using the isotopic composition of plant tissue as a biomonitor of atmospheric N exposure.

Chapter 3 details a similar study; however it is scaled up to an urban to rural gradient. This study used similar methods to the road gradient research, but examines N deposition at urban, suburban and rural sites in two metropolitan areas.

TABLE OF CONTENTS

LIST OF TABLES

LIST OF FIGURES

PREFACE

Funding for this research was provided by the Global Change Research Program (United States Forest Service), the Maryland Power Plant Research Program, the Geological Society of America and the University of Pittsburgh School of Arts and Sciences. Thanks to site operators, including Andy Mack & the Carnegie Museum of Natural History Powdermill Nature Reserve; the Allegheny County Health Department; the Westmoreland County Conservation District; and John Hom, Matt Patterson, and Ken Clark of the USFS. Thanks to John Sherwell, Mark Garrison, Anand Yegnan and Surya Ramaswamy for conducting the CALPUFF modeling described in Chapter 2. Thanks to Ernst Conservation Seeds for the generous seed donation.

I would like to acknowledge the people who helped with laboratory and field work for this project. This includes: Jessie Bobrzynski and Andrew McCarty for their tireless efforts grinding plant and soil samples and harvesting bacteria; Dan Bain, for running my samples on the IC; and Luke Fidler, for assistance with sample collection. A very special thanks goes out to the people who helped set up and tear down my sites: Marion Sikora, Emily Elliott and Dave Felix. Thanks again to Marion for helping me for hours on end in the lab, for helping me practice for talks and for being an excellent friend. I would also like to thank my husband, Adam Redling, who on top of helping me with field work, gave me invaluable moral support and love during my time in graduate school and always. Finally, thanks to my committee for comments on this manuscript and for serving on my committee.

1.0 A REVIEW OF NITROGEN AND CARBON ISOTOPIC TOOLS FOR POLLUTION GRADIENT STUDIES

1.1 NITROGEN

While reactive nitrogen is an important plant nutrient, in surplus it can have widespread detrimental environmental and human health effects. Reactive nitrogen includes species of nitrogen that are "biologically, photochemically and radiatively active" [*Galloway et al.*, 2003] and can be rapidly interchanged, including nitrate (NO_3-), nitrite (NO_2-), ammonia (NH_3+), nitric acid (HNO_3) and nitrous oxide (N_2O) [*Galloway et al.*, 2003; *Socolow*, 1999]. Natural sources of reactive nitrogen include lightning and biological fixation. In dynamic equilibrium, inputs of reactive N are roughly equal to outputs of N_2 from denitrification, which balances nitrogen cycling. However, human activities have altered the global nitrogen cycle through the introduction of additional sources of reactive N, including fossil fuel combustion and fertilizer application [*Galloway et al.*, 1995]. Currently, the addition of anthropogenic reactive nitrogen to ecosystems exceeds that from natural sources [*Galloway et al.*, 2004]. Moreover, the rate of N input to terrestrial ecosystems has more than doubled since the industrial revolution, and N input now exceeds the amount of N export from denitrification [*Vitousek et al.*, 1997].

A major source of atmospheric anthropogenic reactive nitrogen is combustion of fossil fuels for energy production[1]. The main product of these reactions is NO, which is produced via two pathways [*Moomaw*, 2002]. The first is through thermal production, in which atmospheric nitrogen (N_2) and oxygen react at high temperatures to produce NO. The amount of NO produced through this pathway is dependent on flame temperature, gas pressure and time of contact between the fuel and the flame [*Turns*, 1996]. The second pathway to produce NO from fossil fuels is through the pyrolysis of organically bound nitrogen (such as amines or volatile ammonia) in the fuel. Once NO is released into the atmosphere it is oxidized to NO_2 within minutes. NO_2 generally persists between 1 and 5 days in the troposphere, and most NO_2 deposits on surfaces within hours to days [*Galloway et al.*, 2003]. This leads to a heterogeneous distribution throughout the landscape. Accordingly, anthropogenic reactive nitrogen concentrations are usually much higher in polluted urban environments.

Once generated in the atmosphere, NO_2 is quickly transferred to other nitrogen pools. For example, in the atmosphere it is further oxidized into other species, including N_2O_5 and HNO_3. This oxidation is the main mechanism removing reactive N from the atmosphere, as it combines with water to form acidic precipitation [*Moomaw*, 2002]. When combined with water, oxidized N compounds (like HNO_3) dissociate into NO_3- and NO_2-, and become incorporated into soil, surface and ground water supplies. In addition, biota plays a role in N cycling; denitrifying bacteria reduce reactive N back to gaseous N_2O and N_2, and microbes convert organic N compounds to ammonia and nitrate (See Figure 1.1). Because reactive N affects atmospheric, terrestrial and aquatic systems and is rapidly cycled between forms, a *single*

[1] Another major source of reactive N is inorganic fertilizer application, most notably ammonium nitrate. However, full discussion of this source is beyond the scope of this chapter, which focuses on atmospheric fossil fuel emissions.

molecule can have widespread negative ecological effects in a short time period [*Galloway et al.*, 2003].

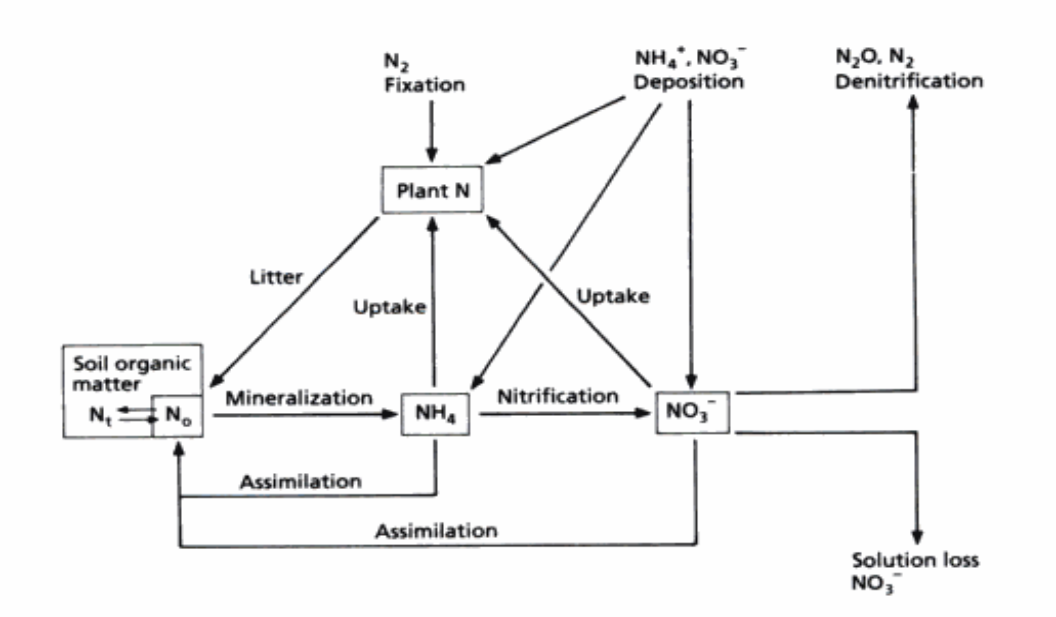

Figure 1.1: The Nitrogen Cycle. From Nadelhoffer and Fry (1994). Various N pools within a forest ecosystem and the associated processes transforming N between pools.

1.1.1 Reactive nitrogen and human health

High concentrations of ambient atmospheric NO_2 can directly harm humans, causing respiratory illness, asthma and increased susceptibility to infection [*Wolfe and Patz*, 2002]. NO_2 in the body acts as a strong oxidant; it can lead to toxicity in lung cells through peroxidation of cell membrane lipids and proteins. This increases cell permeability, leading to injury and cell death [*Wolfe and Patz*, 2002]. NO_2 can also reduce the effectiveness of alveolar macrophages, which increases susceptibility to bacterial and viral infections through a lowered immune response [*Wolfe and Patz*, 2002]. Asthma and other pre-existing respiratory conditions are also aggravated by high levels of NO_2 [*Smith et al.*, 2000]. Moreover, photochemical reactions between NO or NO_2 (collectively NO_x) and natural or man-made volatile organic compounds

leads to the formation of ground level ozone, which can cause inflammation of respiratory passages and decrease lung capacity [*Koren and Utell*, 1997]. This is especially dangerous to people with lung disease and the elderly. In addition to human health effects, ozone can reduce visibility and damage plant tissue.

High NO_3- and NO_2- concentrations in drinking water can also have detrimental impacts to human health. Excess nitrate and nitrite in the body can cause methoglobinemia (blue baby syndrome), wherein nitrate and nitrite ions inactivate hemoglobin in the blood by oxidizing the iron in hemoglobin from Fe^{2+} to Fe^{3+} [*Knobeloch et al.*, 2000]. This bond between nitrite/nitrate and hemoglobin is strong enough that O_2 and CO_2 cannot break it. This lowers the oxygen carrying capacity of the blood, resulting in tissue hypoxia and can lead to coma and/or death. Infants are particularly vulnerable to this condition. Elevated nitrate concentrations have also been linked to stomach, bladder, ovarian and liver cancers because of the formation of N-nitroso carcinogens in the body after exposure to high levels of nitrate [*Weyer et al.*, 2001].

1.1.2 Reactive nitrogen and environmental health

N_2O is produced by partial denitrification of NO_3- by bacteria. It is a naturally formed, stable gas and is well-distributed throughout the troposphere and into the stratosphere. Excess N_2O is often formed when denitrification rates increase with human additions of NO_3- and NO_2- to terrestrial and aquatic systems. When N_2O enters the stratosphere, it acts as a powerful greenhouse gas. It has a global warming potential ~200 times that of CO_2 [*Wolfe and Patz*, 2002] and can thus contribute significantly to global climate change. In addition, N_2O is a catalyst in the chlorine and bromine reactions that destroy stratospheric ozone [*Wolfe and Patz*, 2002], increasing UV radiation reaching the Earth's surface.

The addition of reactive N into terrestrial ecosystems through dry or wet deposition can alter ecosystem structure and function. Most terrestrial ecosystems are naturally N-limited, so when excess reactive N is added to a system, it is initially taken up by biota. This tends to increase net primary productivity, especially in forests. However, with continued inputs of reactive N, many systems eventually become "N saturated" [*Aber et al.*, 1998]. At this point, N inputs to the forest exceed that which biota can use, and it is exported as both solute and gas fluxes. With additional inputs, forest health can decline and dissolved inorganic nitrogen export increases. Symptoms of an N-saturated ecosystem include decreased tree growth and increased tree mortality, decreased net primary productivity and increased nitrification and leaching losses [*Aber et al.*, 1998]. In addition, nitrogen to carbon ratios within plant tissue can be altered, leading to nutrient imbalances. This can cause increased plant susceptibility to other stresses, such as frost, insects and ozone damage [*Matson et al.*, 2002]. In addition, N-tolerant plants can become dominant in N-saturated forests, which can lead to decreased biodiversity [*Vitousek et al.*, 1997] and promote the growth of invasive species [*Townsend et al.*, 2003].

Acidification of terrestrial and aquatic ecosystems can also disrupt ecosystem function. Acid precipitation, caused by the dissolution of HNO_3 and NO_x into rainwater, can decrease the pH of surface waters, destroying habitat and causing population decline of sensitive species. It can also leach base cations and metals from sediments and soils into water, which removes important plant nutrients from the soil and enhances toxic metal availability [*Rabalais*, 2002].

Reactive N also affects surface waters through eutrophication. Excess reactive N acts as a fertilizer for phytoplankton. Algal blooms, including noxious and toxic algal blooms that present a human health risk [*Rabalais*, 2002], are common in waters characterized by excess N loading. Increased water column turbidity from algal shading consequently alters habitat

structure and damages populations of sensitive species. Decomposing algae can also cause hypoxia and anoxia to develop in bottom waters, which can degrade benthic populations, shift food webs and cause a loss of aquatic biodiversity [*Howarth et al.*, 1996]. Continued inputs of N further degrade the aquatic system, leading to widespread permanent or seasonal hypoxia in large water bodies. For example, both the Gulf of Mexico and the Chesapeake Bay experience "dead zones" every summer, when widespread hypoxia develops, prohibiting aquatic organisms from inhabiting these zones.

1.1.3 Determining sources of nitrogen pollution

While the consequences of excess N pollution are well characterized, the mechanisms for N dispersal through the environment are poorly understood. For example, it is difficult to distinguish between the sources of reactive N in any given location, which is necessary for developing regulation strategies for these pollutants. For example, point and non-point sources of air pollution are regulated differently under the Clean Air Act. About 2/3 of anthropogenic atmospheric NO_x are estimated to come from fossil fuel combustion from both mobile (e.g. automobiles) and stationary sources (e.g. electrical generating units) [*Galloway et al.*, 2004]. Vehicular sources account for an estimated 34% of NO_x pollution in North America [*Bradley and Jones*, 2002], and 54% in the Eastern U.S [*Butler et al.*, 2005]. Automobiles may also be an important source of NH_3 due to three-way catalytic converters [*Cape et al.*, 2004; *Fraser and Cass*, 1998; *Sutton et al.*, 2000]. The variety of atmospheric reactive N sources can lead to ambiguity in how to manage these pollutants. For example, a roadway is not considered a stationary source of pollution; rather it is a conglomeration of many non-point sources.

Furthermore, reactive N is prevalent in natural systems. It is important to be able to differentiate and quantify anthropogenic vs. natural sources, as well as the different anthropogenic sources, in order to develop reduction strategies and management plans.

One of the ways we can distinguish the sources of reactive N to a given ecosystem is through stable isotope analysis of atmospheric and terrestrial N compounds.[2] Major N sources have distinct isotopic signatures, which can be used to aid in the differentiation of sources (See Table 1.1).

Table 1.1 Isotopic values of varied atmospheric and terrestrial N sources

Source	δ^{15}N Value, ‰	Citation
Tailpipe Exhaust, high load	+3.7 to +5.7	Moore, 1977
Tailpipe Exhaust, idle	-13 to -2	Heaton, 1990
Coal-fired Power Plant NO_x	+6 to +13	Heaton, 1990
Coal-fired Power Plant NO_x	+10 to +19	Felix, submitted
Soil NO_x	-15 to -5	Ammann, 1999
Soil NO	-19 to -49	Li, 2008
Animal Waste NH_3 Emissions	<<0	Stewart, 1995

For example, atmospheric mobile and stationary sources of N compounds have varied isotopic signatures. Coal combustion δ^{15}N-NO_x values range from +6 to +20‰ [*Felix et al.*, submitted; *Heaton*, 1990]. Automobile δ^{15}N-NO_x values range from -13 to -2‰ from idling vehicles [*Heaton*, 1990] and +3.7 to +5.7‰ from vehicles under high load [*Moore*, 1977]. However, δ^{15}N-NO_x values up to +9‰ have been measured near roadways [*Ammann et al.*,

[2] Expressed in δ notation: $\delta = (R_{sample}/ R_{standard} - 1) \times 1000‰$, where R= the molar ratio of heavy to light isotopes and ‰ is parts per thousand. The standard refers to conventional international standards, which is atmospheric N_2 for nitrogen isotopes.

1999]. Biogenic soil δ^{15}N-NO emissions have more negative values of -5‰ to -15‰ [*Ammann et al.*, 1999]. More recent work by Li [2008] reports values for soil NO are even lower, between -19 and -49‰. NH_3 emissions from animal waste sources and agriculture are generally depleted, with values much lower than 0‰ [*Koopmans et al.*, 1996; *G R Stewart et al.*, 1995].

1.1.4 Plants as biomonitors of atmospheric nitrogen pollution

Another way to monitor the contribution of atmospheric N sources to ecosystems is by measuring the δ^{15}N value of plant tissue; examining the isotopic composition of plant nitrogen can potentially indicate the sources of N to which the plant was exposed during its lifetime. However, a wide variety of factors control the nitrogen isotopic composition of plant tissue [*Högberg*, 1997]. Different forms of N are readily interchangeable and affected by microbial activity within the soil. Furthermore, some nitrogen reactions are reversible, depending, for example, on soil pH and moisture levels. Fractionations can occur during cycling due to microbial activity and physical and chemical processes [*Högberg*, 1997]. This causes distinct spatial patterns of δ^{15}N within soils and vegetation. For example, leaf litter and vegetation tends to be more depleted in ^{15}N, while humus in soil becomes enriched. Soils generally become more enriched with depth [*Nadelhoffer and Fry*, 1994]. While these complexities make using N isotopes somewhat problematic, they could potentially provide useful information about N sources used by plants and fluxes of N within ecosystems. For example, although different types of N are compartmentalized and have varied isotopic compositions, the system average composition will remain relatively consistent unless N fluxes with different isotopic compositions are added to or subtracted from the system [*Högberg*, 1997]. Therefore the

isotopic composition of a system is a function of the fluxes of N into and out of the system [*Nadelhoffer and Fry*, 1994].

The type of nitrogen compound assimilated into plant tissue will also have a direct effect on the plant isotopic composition [*Högberg*, 1997]. Plants generally fall into one of three categories: those which prefer NH_3 exclusively, those which utilize NO_3- and those which can use either type [*Pearson and Stewart*, 1993]. The category depends on the species of plant, its location on the land surface and the amount of either NH_3 or NO_3- available for consumption. Other factors influencing the isotopic composition of plant tissue are the source of the nitrogen, the depth in the soil from which the N is taken up and the influence of mycorrhizal symbioses. Therefore, ^{15}N studies work best when used in experimental settings, in comparisons within ecosystems, or in combination with other stable isotope systems, like oxygen and carbon [*Högberg*, 1997].

The uptake of atmospheric N compounds as a plant nutrient source has long been overlooked; it is commonly thought that rooted plants get most of their nutrients from the soil, including NO_3- from soil water and other forms of inorganic N. However, plants are also able to take up atmospheric N through the leaves. For example, Port and Thompson [1980] found landscape plants grown close to highways in poor soil conditions had elevated levels of N in their tissue, suggesting uptake of N from automobile NO_x. The uptake of atmospheric N compounds has also been demonstrated in chamber fumigation studies and tracer studies using ^{15}N-labelled NO_2 [*Thoene et al.*, 1991], gaseous and particulate NH_3 [*Garten*, 1993] and HNO_3 [*Padgett et al.*, 2009]; all of these studies showed distinct isotopic changes in plant N after exposure. Once inside a plant, ^{15}N can be distributed to all parts (except mature leaves) very rapidly [*Rowland et al.*, 1987].

Part of the reason atmospheric sources of N to plants have not been considered important is because gaseous NO_2 and NO have long been associated with harming plant tissue. For example, studies have found that NO_2 is damaging to plant cuticles and can cause decreased photosynthesis through lowering stomatal conductance [*Wellburn*, 1990]. However, these harmful effects are confounded by the presence of other pollutants, such as sulfate aerosols, ozone and free radicals [*Wellburn*, 1990]. Furthermore, NO_2 and NO must be evaluated separately, as one is far more harmful than the other. NO and NO_2 enter a plant through open stomata during photosynthesis. When they come in contact with extracellular water covering plants cells, these compounds combine with the water, forming HNO_2 and HNO_3, respectively, and dissociating to produce NO_2- and NO_3-, respectively. Through this pathway, NO generally forms NO_2- and NO_2 forms NO_3-. Plant cells readily use NO_3- for building amino acids and plant metabolism (after reducing it with the nitrate reductase enzyme). NO_2-, on the other hand, inhibits plant function, and thus acts as a phytotoxin [*Wellburn*, 1990].

Another reason atmospheric N has been overlooked as a nutrient source to plants is that in natural systems, it is not typically available in sufficient quantities to become an important source. For example, Hanson et al. [1989] calculated the average annual input of nitrogen to forested systems from NO_2 deposition was around 1.9 kg ha^{-1} yr^{-1}, which only represents about 1-3% of a tree's annual nitrogen requirements. In contrast, the same study reported that NO_2 deposition in urban areas is up to 12 kg ha^{-1} yr^{-1} of, which could increase the amount of plant uptake of atmospheric NO_2 [*Hanson et al.*, 1989]. However, these estimates of N deposition are very conservative, because NO_2 is not the only reactive N species available for foliar uptake. Hutchinson et al. [1972] estimated that forest canopies could take up as much as 20 kg ha^{-1} yr^{-1} of NH_3. In addition, particulate HNO_3 can be an important source of atmospheric N in rural

areas, far from NO_2 sources [*Bytnerowicz et al.*, 1987]. In comparison, gaseous HNO_3 has a high deposition velocity, causing it to rapidly settle out of the atmosphere onto plant foliage. The addition of these other reactive N compounds to previous estimates for nitrogen deposition increases estimates for total N deposition substantially. For example, Pearson and Stewart [1993] estimate total N deposition ranging from 5 to 50 kg ha^{-1} yr^{-1} in rural locations in Europe. This estimate ranges even higher in areas near local pollution sources, such as intensive agriculture or near coal-fired power plants.

1.1.5 Examples of the use of stable isotopes of nitrogen in pollution studies

Despite the fact that many plants primarily receive N nutrition through the roots and there are complexities in interpreting $\delta^{15}N$ values in plant tissue, several studies have demonstrated that the $\delta^{15}N$ of plant tissue reflects the $\delta^{15}N$ of atmospheric sources. Stewart et al. [2002] found that plants in an extremely polluted urban site had low $\delta^{15}N$ values relative to plants in a rural area several kilometers away, indicating that the cause of the low $\delta^{15}N$ values in urban plant tissue was exposure to atmospheric pollutants with lower $\delta^{15}N$ values. The main source of pollution at the urban site was NH_3 from a petrochemical plant, with measured $\delta^{15}N$ values of emissions around -40‰. Epiphytes, which are plants that rely exclusively on atmospheric sources of N for nutrients, had especially low $\delta^{15}N$ values compared to soil-grown plants [*G Stewart et al.*, 2002]. In comparison, historic plant samples from the urban site were more enriched than modern samples; the historic plants were grown prior to the onset of pollution from the petrochemical plant.

Not all studies of plant isotopes in polluted areas reveal depleted $\delta^{15}N$ values; many report enriched values (e.g., [*Gebauer and Schulze*, 1991; *Högberg*, 1997; *Jung et al.*, 1997]). Studies suggest that relatively high $\delta^{15}N$ values in plants recovered from polluted sites result from uptake of NO_x from coal burning power plants and automobiles. The higher isotope values for this source (~+6 to +13) are thus transferred to plant tissue at more polluted sites. For example, Jung et al. [1997] measured $\delta^{15}N$ in plant tissue in highly polluted urban locations and rural areas with low NO_x emissions. The $\delta^{15}N$ values differed by ~10‰, with plants from urban locations having more positive values.

Some studies have examined N isotope compositions of vegetation using much smaller gradients. For example, Ammann et al. [1999] measured the $\delta^{15}N$ of atmospheric NO_x within several hundred meters of a highway and the isotopic composition of tree tissue at varying distances from the road. They found that NO_x had high $\delta^{15}N$ values, around +5.7‰. The plant tissue reflected the affects of this atmospheric source; tree needles near the road had $\delta^{15}N$ values 2‰ higher than samples farther from the road. Saurer et al. [2004] conducted a similar study along this same gradient using tree rings. They report tree tissue near the road had more positive N isotope compositions, reflecting the automobile source. The use of tree rings in this study recorded the history of the area as well; tree ring $\delta^{15}N$ values became higher after the construction of the highway, which was about 40 years before the study.

This application can also be used to compare different amounts of pollution (rather than distance from the source). Pearson et al. [2000] conducted a study comparing $\delta^{15}N$ of moss tissue along roadways with varying traffic density. They showed that mosses exposed to varying levels of traffic density had different nitrogen isotopic compositions and levels of heavy metals in their tissues. Mosses near major roadways had higher $\delta^{15}N$ values, indicative of an uptake of

N compounds from an automobile source. Near-roadway plants also had much higher concentrations of heavy metals, including lead and zinc.

It is important in these studies that the actual source of N is measured for isotopic composition, as this will help interpret the results. Measuring the natural abundance of ^{15}N in a plant will not directly tell us whether it is exposed to pollution or not. It is crucial to examine the concentration and the isotopic composition of the gaseous species of N which is the primary pollutant. In addition, this can help account for mixing of varied sources with different $\delta^{15}N$ values that may be affecting the plant tissue composition, including both atmospheric and soil water sources.

1.2 CARBON

1.2.1 Urban areas as proxies for global climate change

CO_2 is important in a global context; it is a major greenhouse gas that contributes to global climate change. The Intergovernmental Panel on Climate Change predicts that global concentrations of CO_2 will rise to between 500 and 1000ppm by 2100, leading to a projected global temperature increase of 1-3.5°C [*Trenberth et al.*, 1996]. Due to high local levels of anthropogenic fossil fuel combustion from both mobile and point sources, urban areas are key contributors to atmospheric carbon dioxide (CO_2) emissions. Several studies have established the existence of a CO_2 "dome" in urban locations, where concentrations of CO_2 are higher in cities than adjacent rural areas [*Idso et al.*, 2001; *Pataki et al.*, 2007; *Ziska et al.*, 2003]. Furthermore, the well documented urban "heat island" effect may be enhanced by higher CO_2

concentrations [*George et al.*, 2007]. The urban "CO_2 dome" may be used as a proxy for global climate change scenarios; elevated CO_2 concentrations and temperatures in urban areas are analogous to conditions expected globally with continued inputs of CO_2 into the atmosphere.

CO_2 emissions in urban areas are heavily influenced by local fossil fuel combustion. For example, diurnal variations in CO_2 concentration often track regional traffic patterns, with higher concentrations during rush hour [*Nasrallah et al.*, 2003; *Velasco et al.*, 2005]. CO_2 concentrations have also been shown to follow a seasonal pattern, with higher concentrations occurring in the winter and summer, corresponding to increased power generation due to heating and air-conditioning [*Blasing et al.*, 2005; *Pataki et al.*, 2007]. However, it is difficult to track the quantity of CO_2 emissions coming from each source using concentration data alone; this information could be useful for developing regulation and management strategies of greenhouse gas emissions in urban areas.

1.2.2 Vegetation as a sink for CO_2

Increased CO_2 concentrations in urban areas have implications for vegetation in urban ecosystems. From a management perspective, understanding the nutrient dynamics of vegetation in urban ecosystems is critical to understanding carbon budgets. For example, climate change may increase the growing season, leading to alterations in plant phenology, which can disrupt ecosystem function [*Fitter and Fitter*, 2002]. However, while vegetation may represent an important sink for excess carbon, it is difficult to quantify how urban vegetation responds to increased CO_2 levels. Furthermore, it is poorly understood how the spatial and temporal variations in CO_2 concentrations from varied sources affect vegetation. Chamber studies have

shown increases in plant biomass with increased concentrations of CO_2 [*Kimball et al.*, 1993; *Wittwer and Strain*, 1985], suggesting that plants are an important sink of excess carbon. However, in natural systems, other confounding factors, such as disturbance, competition and nutrient availability, may prevent excess growth and carbon uptake. For example, Ziska et al. [2004] found a 115% increase in initial plant productivity at urban sites along an urban to rural transect in Baltimore, MD as a result of increased CO_2 and temperature in the urban location. However, after three years, the numbers of annual herbaceous vegetation decreased at the urban site, leading to an overall decrease in productivity [*Ziska et al.*, 2007].

1.2.3 Using stable isotopes of carbon to source CO_2

Major sources of CO_2, including fossil fuel combustion byproducts and biogenic emissions, have distinct isotopic signatures (see Table 1.2). The $\delta^{13}C$ value of global ambient atmospheric CO_2 is -8‰ [*Keeling et al.*, 1989]. This is lower than $\delta^{13}C$ values measured in atmospheric gas of ice cores age-dated to 250 years before present, which are approximately -6.3‰ [*Marino and McElroy*, 1991]. In comparison, $\delta^{13}C$ values of vehicular CO_2 and coal combustion are between -27‰ and -25‰ [*Clark-Thorne and Yapp*, 2003]. The global atmospheric $\delta^{13}C$ decrease is a function of fossil fuel combustion; adding CO_2 depleted in $\delta^{13}C$ has caused the global average $\delta^{13}C$ values to drop since the Industrial Revolution [*Keeling*, 1979]. This trend is also evident at a local scale: environments with major CO_2 inputs from fossil fuel combustion have lower $\delta^{13}C$-CO_2 values than the global average [*Pataki et al.*, 2003]. Therefore, urban areas are generally expected to have lower $\delta^{13}C$ values of CO_2 relative to rural areas due to elevated CO_2 concentrations from fossil fuel combustion.

Table 1.2 Carbon isotopic signatures of CO_2 sources and plant tissue		
Source	**$\delta^{13}C$ value, ‰**	**Citation**
Coal combustion	-24.1	Blasing, 2005
Oil combustion	-26.5	Blasing, 2005
Natural gas combustion	-44.0	Blasing, 2005
Automobile exhaust	-27.0	Clark-Thorne, 2003
Global background	-8.0	Keeling, 1989
C3 Plant tissue	-30 to -22	Farquhar, 1989
C4 Plant tissue	-14 to -10	Farquhar, 1989

1.2.4 Studies using stable isotopes of carbon in plant tissue

Carbon isotopes have long been used as a tool to study plant function [*Farquhar et al.*, 1989]. For example, carbon isotopes can be used to differentiate between C3 and C4 plants [*O'Leary*, 1981]. As CO_2 is incorporated into plant tissue during photosynthesis, the carbon isotopes undergo fractionation, resulting in plant tissue $\delta^{13}C$ values which are lower than $\delta^{13}C$-CO_2 [*O'Leary*, 1981]. The fractionation is a function of diffusion of CO_2 through the stomatal pore, diffusion of CO_2 in air through the boundary layer of the stomata, diffusion of dissolved CO_2 through water and the type of photosynthetic enzyme used by the plant [*Farquhar et al.*, 1989]. C3 and C4 plants each use a different photosynthetic enzyme to convert CO_2 into sugars (Ribulose bisphosphate carboxylase in C3 plants and Phosphoenolpyruvate carboxylase in C4 plants); therefore C3 and C4 plants experience different carbon isotope fractionation during photosynthesis [*O'Leary*, 1981]. $\delta^{13}C$ values for C3 and C4 plants are about -27‰ and -13‰, respectively. Other factors that can influence $\delta^{13}C$ values of plant tissue include fertilization, the plant part measured (stem vs. roots), temperature, salinity and CO_2 concentration [*O'Leary*, 1981].

Another factor influencing $\delta^{13}C$ composition of plant tissue is CO_2 source. Previous studies have shown that the $\delta^{13}C$ composition of plant tissue reflects the $\delta^{13}C$ of ambient CO_2 [*Farquhar et al.*, 1989]. As such, tracer studies using ^{13}C-depleted CO_2 can be implemented to study plant physiology. For example, Pepin and Korner [2002] conducted a free air CO_2 enrichment study, in which CO_2 was pumped into forested plots in order to explore how tree canopies respond to increased CO_2 concentrations. Because the pumped-in CO_2 was derived from fossil fuel sources, it had a more negative $\delta^{13}C$ value than ambient atmospheric CO_2. As a result, plant tissue $\delta^{13}C$ values decreased during the course of the study. The authors used measurements of $\delta^{13}C$ in the plant tissue to determine long-term CO_2 concentrations across their study area. CO_2 concentrations derived from plant tissue isotope values were well-correlated with measured CO_2 concentrations [*Pepin and Körner*, 2002].

Another novel use of carbon isotopes in plant tissue is determining varying CO_2 sources to plant tissue along a spatial gradient, though very few studies to date have used this technique. Most notably, Lichtfouse *et. al*. [2002] examined $\delta^{13}C$ of grasses along an urban to rural gradient. CO_2 concentrations varied along the gradient; urban areas had higher CO_2 concentrations due to fossil fuel emissions. Because fossil fuel CO_2 emissions have lower $\delta^{13}C$ values than ambient atmospheric CO_2, the authors hypothesized that average $\delta^{13}C$ value in urban areas would be lower than surrounding areas, and this would be reflected in plant tissue. Their results supported this hypothesis; $\delta^{13}C$ of grass tissue was ~5‰ lower in urban areas [*Lichtfouse et al.*, 2002].

1.3 CONCLUSIONS

Anthropogenic reactive nitrogen and carbon dioxide can have fundamental consequences for human and environmental health. Reactive N can negatively affect all global systems, including atmospheric, aquatic, terrestrial and biotic systems. In particular, different forms of reactive N can impact human health, potentially causing respiratory disease, cancer and other health effects. CO_2 contributes to global climate change and thus is a factor in observed shifts in temperature, sea level, and weather patterns around the globe.

As such, it is necessary to regulate the varied sources of reactive N and CO_2, including emissions from automobiles and power generation units. However, this becomes complicated under the Clean Air Act, which regulates sources of pollution differently, and cannot account for natural sources of reactive N and CO_2.

One of the ways to ameliorate this issue is to differentiate the sources of reactive N and CO_2 to any given location. This may be accomplished using stable isotopes of N and C in various pools and comparing those with known or measured source values. One of the problems with this method is the complexity of N and C cycling within environments; the varied pathways and transformations can obscure the interpretation isotopic values in natural systems. This issue may be overcome by using N and C in combination with other stable isotope systems like oxygen, or by using controlled experimental settings and/or conditions.

Plants represent an important sink for N and CO_2, and can be key to determining the fate of varied N and CO_2 sources to the environment. Plant uptake of the varied atmospheric N species has been documented in both chamber studies and in the field. Furthermore, the isotopic value of plant tissue has been repeatedly shown to reflect the isotopic signature of the

atmospheric source of nitrogen and CO_2. Eventually, isotopic studies of plant tissue may be used as a tool to quantify the levels of different sources of N pollution affecting plants.

The following chapters describe two studies which use the isotopic composition of plant tissue ($\delta^{13}C$ and $\delta^{15}N$) to determine the impact of anthropogenic pollution sources on local vegetation. Each study was sited along a pollution gradient; a highway road gradient in Chapter 2 and two urban to rural gradients in Chapter 3.

2.0 ISOTOPIC INVESTIGATION OF DRY NITROGEN DEPOSITION ALONG A HIGHWAY ROAD GRADIENT

2.1 INTRODUCTION

NO_x emissions from vehicular sources can create corridors of increased air pollution near highways. For example, studies document elevated atmospheric NO_x concentrations within hundreds of meters of roadways [*Gilbert et al.*, 2007; *Roorda-Knape et al.*, 1998; *Singer et al.*, 2004]. However, there is limited understanding of the effects of these emissions on the surrounding environment. Because vehicle emissions comprise ~50% of Eastern U.S. NO_x emissions [*Butler et al.*, 2005], it is critical to identify the fate and impact of automobile emissions on near-road ecosystems. Atmospheric NO_x and other N pollutants (HNO_3 and NH_3) have relatively short atmospheric lifetimes (1 to 8 days) and high deposition velocities, causing them to deposit near their sources as particulates and aerosols in dry deposition [*Kirchner et al.*, 2005; *Moomaw*, 2002]. Unlike emissions from regional air pollution sources (e.g., smoke stacks), dry deposition from vehicles can deposit within 10s to 100s of meters from roadways [*Cape et al.*, 2004; *Kirchner et al.*, 2005]. This spatial pattern of concentrated nitrogen deposition has implications for near-road environments. For example, storm water infrastructure can channel near-road deposition directly into surface water. Excess nitrogen can also have adverse effects on near-road plant communities; studies document defoliation and changes in

community structure due to nitrogen pollution near roadways [*Angold*, 1997; *Bernhardt-Römermann et al.*, 2006; *Bignal et al.*, 2007].

Most national pollution monitoring facilities in the U.S. (such as the National Atmospheric Deposition Program and Clean Air Status and Trends Network (CASTNET)) are intentionally located in rural areas, far from major pollution sources and transportation corridors, in order to monitor regional air pollution trends. While this provides long term assessment of background N deposition levels, the location of these sites likely underestimates total N deposition to the landscape. Because dry nitrogen deposition from automobiles can deposit locally, the spatial distribution of wet and dry nitrogen deposition monitored at these sites may not take into account automobile pollution. Previous research has shown that N deposition from these sites reflects NO_y derived primarily from stationary sources instead of mobile sources [*Elliott et al.*, 2007]. Furthermore, neither monitoring network measures atmospheric NO_2 and NO_x concentrations (though they do measure particulate NO_3-, HNO_3 and, at some sites, NH_3). As a result, existing monitoring networks may underestimate NO_y and total nitrogen reaching the land surface, especially in urban areas and near roadways.

This study uses stable isotopes of nitrogen in plant tissue and dry nitrogen deposition to examine the extent of nitrogen loading along a gradient perpendicular to a major highway. Stable isotopes of nitrogen can be an effective tool for tracking the sources of atmospheric nitrogen in precipitation and dry deposition. Major atmospheric NO_x sources exhibit distinct isotopic signatures, which can aid in differentiating emissions that contribute reactive N to gaseous species and wet and dry deposition. For example, coal combustion generates NO_x emissions with $\delta^{15}N$ values ranging from +6 to +20‰ [*Felix et al.*, submitted; *Heaton*, 1990]. In contrast, automobile NO_x is characterized by lower $\delta^{15}N$ values, ranging from -13 to -2‰ from

idling vehicles [*Heaton*, 1990] and +3.7 to +5.7‰ for vehicles under high load [*Moore*, 1977]. $\delta^{15}N$ values of biogenic soil NO emissions are lower than fossil fuel sources with values between -19‰ and -49‰ [*Li and Wang*, 2008].

This study examines the effects of increased roadway N deposition on local vegetation by using the isotopic composition of plant tissue as a biomonitor of atmospheric N exposure. While plants assimilate most nitrogen through roots, atmospheric NO_x, HNO_3 and NH_3 uptake through leaves can also be an important nutrient source to plants [*Wellburn*, 1990]. This is evidenced by studies that document $\delta^{15}N$ composition of plant tissue reflects $\delta^{15}N$ of atmospheric NO_x [*Ammann et al.*, 1999; *Pearson et al.*, 2000; *Saurer et al.*, 2004]. By coupling plant tissue isotopic composition with concentration and isotopic composition of atmospheric reactive nitrogen, we assess the extent of N transport in near-road environments, the fate of this reactive N, and the potential influence on local vegetation.

2.2 EXPERIMENTAL SECTION

2.2.1 Site description

The road gradient was located at the Carnegie Museum of Natural History Powdermill Nature Reserve near Donegal, Pennsylvania (USA) (N 40° 07' 42.2"; W 79° 17' 11.7"). The gradient was situated in a meadow that abuts Interstate-76, a five-lane highway that receives ~33,300 annual average vehicles per day [*Pennsylvania_Department_of_Transportation*, 2009] and has a speed limit of 104 km per hour (65 mph). Sites along the gradient were established at 2, 12, 30, 90, 188 and 460 meters away from the roadway (Figure 2.1).

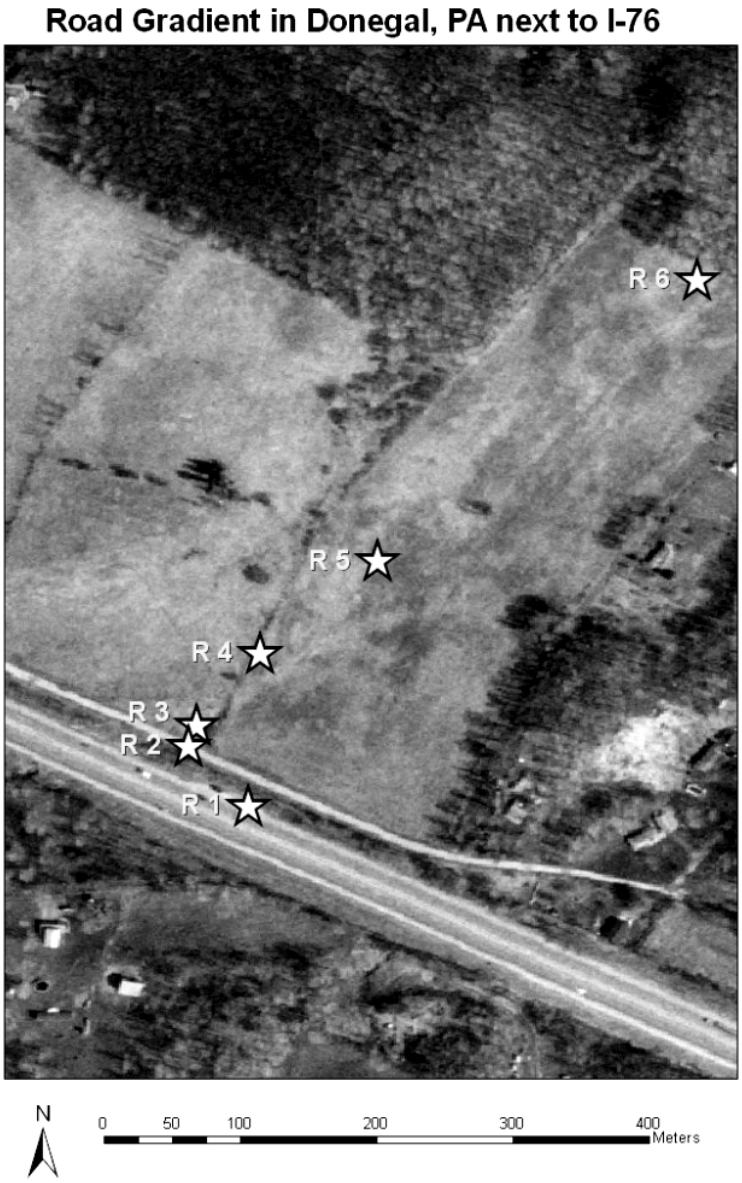

Figure 2.1: Map of the road gradient. Aerial photograph of the road gradient site with sampling locations marked by stars.

2.2.2 Plant sampling and analysis

Each site contained two pots of plants, one *Agrostis perennans* (Autumn Bentgrass) and one *Panicum virgatum* (Switchgrass). The 12m site contained two *Panicum virgatum*; it did not

contain *Agrostis perennans* due to plant mortality at that site. No plants were sited at 2m because of highway right-of-way restrictions. Each pot contained approximately fifty individual plants. Pots were doubled to prevent water loss, intrusion of native soil and root growth through the bottom of the pots. Because plant roots could not access soil beyond the pot exterior, it was assumed that plants only received nutrients from the soil in the pot and atmospheric deposition. All plants along the gradient were grown from seed in the same location, ensuring that all plants would start with similar isotopic compositions. Likewise, all the plants were grown and eventually re-potted in well-homogenized potting soil. With these controls in place, as the plants gained biomass throughout the summer, they should acquire the isotopic signature of the reactive N and CO_2 of the surrounding air in which they were growing. By controlling the soil media, using multiple individuals and effectively restricting the plants to their pots, the amount of isotopic variability between individual plants prior to exposure was limited. Throughout the study period, the grasses produced new biomass after each cutting. Plants were sampled prior to deployment and then monthly from July through October 2008. In addition, soil was sampled monthly concurrent with plant sampling. Samples were cut with scissors, washed with Milli-Q water and placed in individual bags. Approximately 100 grams of soil were spooned out of the pots from a depth of 2-5 centimeters and placed in individual bags. All samples were transported on ice to laboratories at the University of Pittsburgh and were subsequently frozen to prevent tissue breakdown. Samples were later freeze-dried, ground with a commercial coffee grinder and mortar and pestle and packed into tin capsules for isotopic analysis. Isotopic analysis was conducted in a EuroVector high temperature elemental analyzer connected to a GV Instruments Isoprime Continuous Flow Isotope Ratio Mass Spectrometer (CF-IRMS).

2.2.3 Gas sampling and analysis

NO_2 and HNO_3 were collected with passive diffusion samplers at each site. This is an effective and inexpensive method for monitoring dry deposition [*Bytnerowicz et al.*, 2005] and isotopic composition [*Elliott et al.*, 2009] of nitrogen compounds. Samplers for NO_2 were purchased from Ogawa, USA, and samplers for HNO_3 were similar to the USDA Forest Service design described by Bytnerowicz *et al.* [2005]. These samplers collect atmospheric species on a chemically reactive filter pad. Each gas requires a different filter. For NO_2, pre-coated filters purchased from Ogawa, USA were used, whereas HNO_3 was collected using 47mm nylon filters (Pall Corporation). Samplers were deployed for one month intervals, allowing adequate material for analysis to collect. Each sampler holds two filters, which ensures that enough material is collected each month to perform both concentration measurements and isotopic analysis of each species. Each month the filters were changed in the field at the same time grasses were sampled. Exposed filters were loaded into centrifuge tubes and frozen until analysis. In addition, we used a field and laboratory blank to determine background levels of deposition on the filters prior to deployment. Missing data points included the 2m and 12m sites in July (NO_2 and HNO_3) and the 30m site in August (NO_2) due to highway right of way restrictions and vandalism.

For concentration measurements of NO_2 and HNO_3, each filter was eluted with 5mL of Milli-Q water to produce NO_3- and NO_2-. The eluant was injected into a Dionex ICS2000 Ion Chromatograph. For isotopic analysis of NO_2 and HNO_3 the second filter of each sample was eluted in 5mL of Milli-Q water. The bacterial denitrification method was used to convert the eluted nitrite and nitrate into 10 nanomoles of N_2O gas [*Casciotti et al.*, 2002; *Sigman et al.*, 2001]. The resulting gas was introduced into a GV Instruments Isoprime CF-IRMS. Samples

with eluant concentrations less than 0.23 mg/L were not run for isotopic analysis due to insufficient sample mass. This included four NO_2 samples: the 188 and 460m sites from July and the 90 and 188m sites from August.

While it is extremely difficult to directly measure dry deposition and the associated deposition velocities, concentrations on passive samplers can be used to estimate N flux. In this study, we estimated flux using two methods. For the first estimate, we used the method described by Golden *et al*. [*Golden et al.*, 2008], hereafter referred to as the "Golden method" in which

$$F = (C \times v) / (a \times d)$$

where F is flux, C is the concentration measured in filter eluant, v is elution volume, a is the effective filter area and d is the number of days the filter was exposed. For the second estimate, we used a method described by Roadman *et al*. [*Roadman et al.*, 2003], hereafter referred to as the "Roadman method" in which

$$C = (m / t) / M$$

$$F = C \times V_d$$

where C is the average ambient concentration, m is the mass of N on the filter, t is the time the filter was exposed, M is the mass transfer coefficient, F is flux and V_d is the deposition velocity. For the Roadman method calculations, mass transfer coefficients derived from the literature were used for each type of sampler design. For the NO_2 sampler design, there were two mass transfer coefficients reported, 12.1 cm^3/min [*Tang et al.*, 2001] and 9.5 cm^3/min [*Yu et al.*, 2008], hereafter referred to as the "Roadman low" and "Roadman high" scenarios, respectively. To our knowledge, only one mass transfer coefficient has been reported for the HNO_3 sampler used in

this study (31.855 m^3/hr [*Bytnerowicz et al.*, 2005]). As such, only one flux is calculated using the "Roadman method" for HNO_3.

Deposition velocities for NO_2 and HNO_3 were estimated for the road gradient using the CALPUFF model. CALPUFF (EPA, 2009) is a Lagrangian puff dispersion model, which can simulate the effects of spatial and temporal variations in meteorological data on dispersion, transport, and deposition of pollutant species. Continuous emissions from air pollution sources, such as mobile sources, are simulated by using a series of puffs that are tracked as the puffs are carried downwind. CALPUFF has different options for modeling chemical transformation, depending on the species being modeled. The transformation used in this study simulates the oxidation of NO_x emissions to nitrate as a function of atmospheric stability, ozone concentration, and plume NO_x concentration. CALPUFF then partitions nitrate into gaseous (HNO_3) and particulate ($HNO_3(NH_4)$) forms based on temperature and availability of ammonia. CALPUFF determines dry deposition velocity as a function of land use at the location of each puff, calculates deposition flux based on the amount of mass in the puff and the calculated deposition velocity, and accounts for the total mass of NO_x and NO_3 as the puff is advected and dispersed downwind.

The meteorological data used in this analysis was coincident with the ambient monitoring effort and covered the period between July and November 2008. The surface and upper air meteorological data were obtained from the Pittsburgh Airport (Wban: 94823). A single-point meteorological data set was developed with the meteorological preprocessor called CPRAMMET available with the CALPUFF modeling system. NO_x emissions from the mobile sources along I-76 were calculated using the MOBILE6 emissions estimation model, and the roadway was modeled as a series of 67 volume sources along a stretch of highway approximately

one kilometer to each side of the measurement locations. A receptor grid was developed for the study area covering an area up to approximately one kilometer from the roadway. Hourly concentration and deposition fluxes were calculated for NO_x (NO_2), nitric acid (HNO_3), and particulate nitrate ($HNO_3(NH_4)$) at each receptor for each hour in the study period.

CALPUFF-derived deposition velocities for NO_2 spanned a range (0.0018 m s^{-1} and 0.001 m s^{-1}). For this study, this range in deposition velocities was combined with the range of reported mass transfer coefficients to yield scenarios representing both the highest and lowest potential fluxes for the "Roadman high" and "Roadman low" scenarios, respectively. CALPUFF model estimated deposition velocities for HNO_3 were 0.0035 m s^{-1}. The modeled deposition velocities were in agreement with literature-reported values for NO_2 (0.001 m s^{-1}), but HNO_3 estimated values were lower than literature-reported values (0.04 m s^{-1} for average continental deposition [*Hauglustaine et al.*, 1994] and 0.008-0.033 m s^{-1} modeled for various land types [*Clarke et al.*, 1997]).

The calculations for the Golden and the Roadman methods yield units of kg ha^{-1} yr^{-1}, which is a standard method of reporting N flux. However, as the filter concentrations yielded *monthly* average concentrations for five individual months, the kg ha^{-1} yr^{-1} estimate for each month refers to the estimated amount of N flux in kg ha^{-1} yr^{-1} that would occur for the whole year if the concentrations for that month were consistent throughout the year. We use the kg ha^{-1} yr^{-1} convention in order to compare results from our research with other monitoring studies.

2.3 RESULTS AND DISCUSSION

2.3.1 Reactive nitrogen fluxes and isotopes

Average NO_2 flux for all months ranged from 0.88 to 4.15 kg ha^{-1} yr^{-1} for the Roadman high estimate, 0.38 to 1.31 kg ha^{-1} yr^{-1} for the Roadman low estimate and 0.47 to 2.21 kg ha^{-1} yr^{-1} for the Golden estimate (Figure 2a). The highest average fluxes occurred at the 2m site. Fluxes decreased with distance from the road, and the lowest values were at the 460m site. This pattern indicates that NO_2 is rapidly deposited, within ~100 meters of traffic corridors. This is in accordance with other studies that document elevated concentrations and flux of NO_2 near roadways [*Cape et al.*, 2004; *Kirchner et al.*, 2005].

NO_2 flux also exhibited temporal variation (Figure 3a). The spatial gradient was maintained throughout all months, but with varying intensity. In August NO_2 flux was 3 times higher at the site 2 meters from the road than at the 460 meter site. In September this difference was reduced to only a 2.6-fold increase. In October and November the roadside NO_2 flux was 4 and 4.4 times higher than the 460m site, respectively. The highest estimated flux throughout the study occurred in October at the site 2 meters from the roadway (6.49, 3.46 and 2.83 kg ha^{-1} yr^{-1} with the Roadman high, Golden and Roadman low estimates, respectively). In addition, at all sites, NO_2 flux increased in October and November. This is in agreement with other studies that have documented increases in NO_2 flux in colder months [*Atkins and Lee*, 1998; *Kirby et al.*, 1998]. This may be a function of higher stationary source NO_x emissions during colder months [*Elliott et al.*, 2009], changing oxidation patterns with lower ozone concentrations in winter, or decreased NO_2 uptake by stomata [*Hargreaves et al.*, 1992].

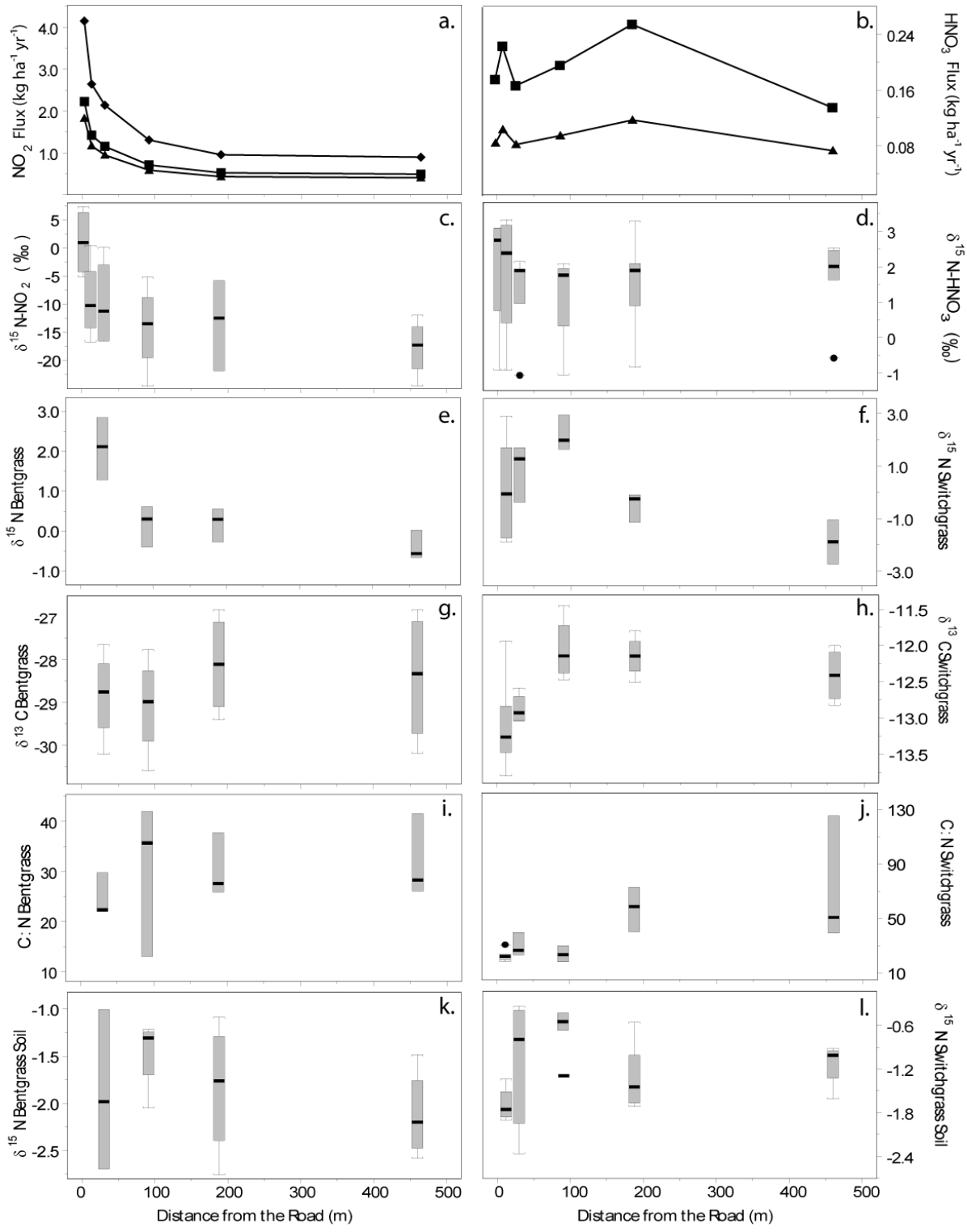

Figure 2.2: Road gradient data. N flux (a- b), atmospheric N isotopes (c-d), plant isotopes (e-h) and C:N ratios (i-j), and soil N isotopes (k-l). For NO_2 and HNO_3 flux, squares are Golden method estimates, triangles are Roadman low estimates and diamonds are Roadman high estimates. Plots c-l are box and whisker plots, in which the box represents the upper and lower

quartile and the whiskers represent the minimum and maximum data point. The center line in the box is the median value. Outliers are shown as black dots with lines through them. Plant data does not include July; as the plants acquired biomass, the N isotopes changed as juvenile plants matured. July data was a mix between seedling values from June and mature plants in August.

HNO_3 flux exhibited different patterns than NO_2 flux. HNO_3 flux was an order of magnitude lower than NO_2, with average flux for all months ranging from 0.13 to 0.26 kg ha^{-1} yr^{-1} for the Golden method and 0.06 to 0.10 kg ha^{-1} yr^{-1} for the Roadman method (Figure 2b). In addition, HNO_3 flux peaked at two sites across the gradient (12 and 188m). Seasonal variation in HNO_3 flux can help explain this spatial pattern of average deposition (Figure 3b). For example, the first peak was caused by a high August flux at 12 m, whereas the second peak was caused by a high fluxes at the 30, 90 and 188 m sites during October and November. As an oxidation product of NO_2, HNO_3 may be formed at a greater distance from the road and thus account for multiple peaks in HNO3 fluxes. Accordingly, HNO_3 fluxes increase in October and November when higher NO_2 fluxes are observed. This contrasts other studies, which have found that HNO_3 concentrations increase in the summer and decrease in the winter, due to changing oxidation patterns in the NO_2 to HNO_3 conversion [*Kondo et al.*, 2008; *Morino et al.*, 2006].

Comparison of the total N flux near the roadway with background levels of N deposition measured at a local CASTNET site reveals an underestimation of N deposition reaching the landscape by regional monitoring networks. Total dry deposition measured at the nearest CASTNET site (Laurel Hill LRL 117, which is 16.09 km from the road gradient) in 2008 was 1.04 kg ha^{-1} yr^{-1}. This included measurements of particulate nitrate, dry NH_4, and HNO_3 [*U.S._EPA_CASTNET*, 2008]. In contrast, at the site 2 meters from the road, the total annual deposition was estimated to be 1.87, 2.38 and 4.21 kg ha^{-1} yr^{-1} for total N (NO_2 plus HNO_3), using the Roadman low, Golden and Roadman high methods of estimation, respectively. This

deposition is based on monthly observed data for the four months of the study, and multiplying it by 3 to account for the entire year. This calculation facilitates a comparison of our observed data with local background levels of dry N deposition. Although this estimate is based on a partial year of data, it is expected that this is a conservative estimate as higher NO_2 concentrations are expected during the winter months. At the site 460 m from the road, which is most likely reflective of the background regional dry N deposition, the total N flux was estimated at 0.44, 0.60 and 0.93 kg ha^{-1} yr^{-1} with the Roadman low, Golden and Roadman high methods, respectively. The Roadman high estimate at this site is the most similar to the flux measured at the CASTNET site; therefore we can use the Roadman high estimate to compare flux along the rest of the gradient. Using the Roadman high estimate for deposition closest to the road, we estimate an additional 3.28 kg ha^{-1} yr^{-1} falling within 2m of the roadway, which is 4 times higher than the CASTNET site. At the site 12 meters from the roadway, the Roadman high estimate was 2.72 kg ha^{-1} yr^{-1}, which is an additional 1.79 kg ha^{-1} yr^{-1} above background (2.6 times higher). These increases in N flux near roadways create corridors of concentrated N deposition across the landscape. This has important implications not only for air quality, but also for water quality and ecosystem health, especially in urban areas where road density is high. Furthermore, our findings highlight the need for longer term monitoring of roadside verges to more accurately characterize total N flux to the land surface.

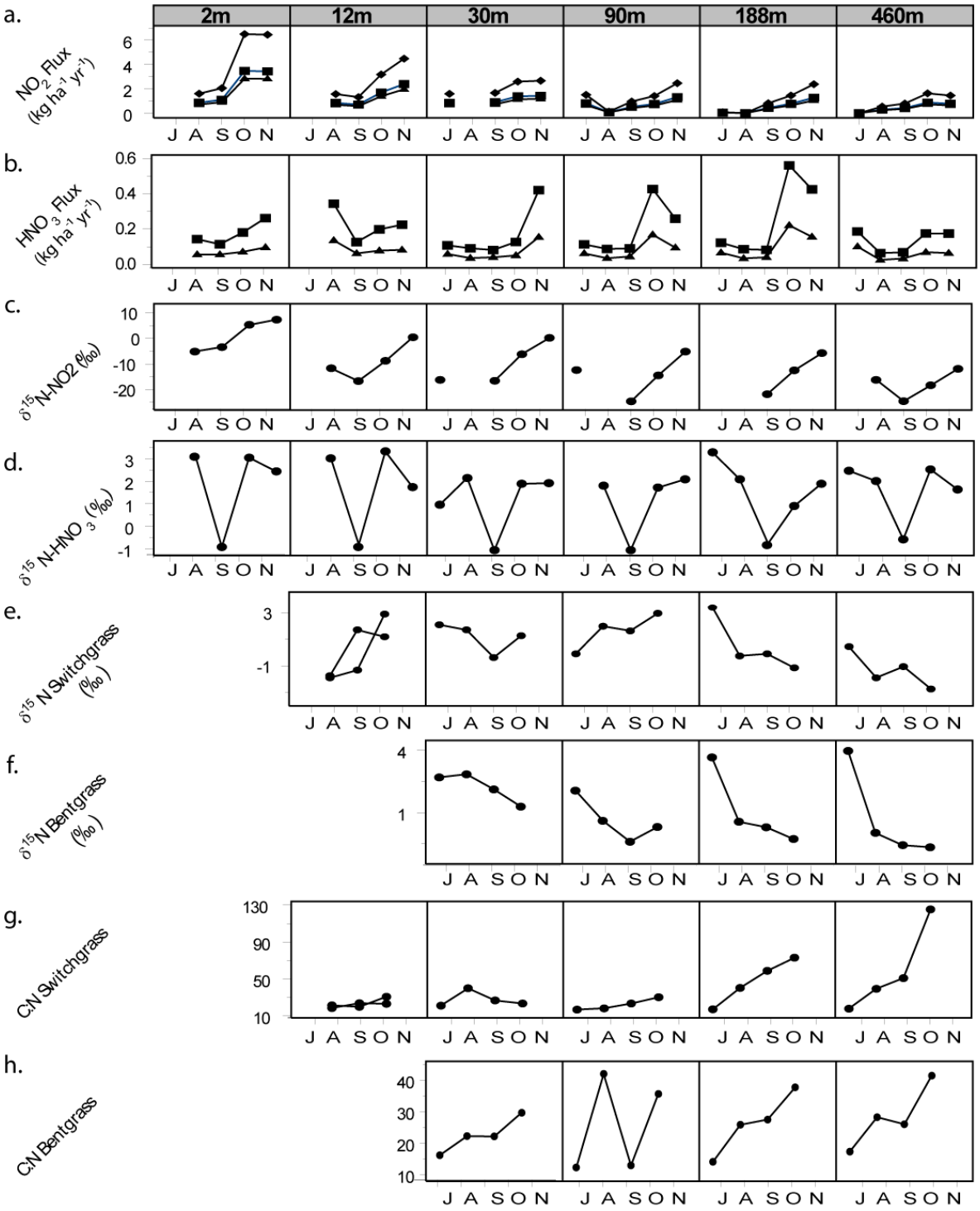

Figure 2.3: Road gradient monthly data: Monthly variations in N flux, atmospheric N isotopes, plant tissue isotopes and plant tissue C to N ratios at each site. For NO_2 and HNO_3 flux, squares are Golden method estimates, triangles are Roadman low estimates and diamonds are Roadman high estimates. For atmopheric N isotopes, missing values (due to low concentrations) are omitted. For plant tissue plots, neither grass was placed at the 2m site. For Switchgrass plots,

the 12m site had two pots of grass; all other sites had one pot. There were no Bentgrass pots at the 12m site.

In this isolated roadside environment we expect the dominant sources of NO_2 and HNO_3 are biogenic and vehicle emissions. N isotopes of each gas can give an indication of which sources contribute to N deposition at each site, and also to the spatial and temporal patterns of deposition coming from vehicle emissions. Vehicular sources have reported $\delta^{15}N\text{-}NO_x$ of +3.7 to +9‰ [*Ammann et al.*, 1999; *Moore*, 1977]. (Lower values were reported by Heaton [*Heaton*, 1990], but these were for idling vehicles. It would be unlikely to see these values from vehicles traveling at interstate highway speed). Biogenic emissions have much lower isotopic values of -19 to -49‰ [*Li and Wang*, 2008].

$\delta^{15}N\text{-}NO_2$ follows a similar spatial pattern as NO_2 flux; mean $\delta^{15}N$ values decrease with distance from the road (Figure 2.2c). The site at 2m from the road had values ranging from -5.1 to +7.3‰. The site 460m from the road had values ranging from -11.9 to -24.6‰. Values at these two sites were significantly different (ANOVA, $p=0.02$). Values at the 2m site were within the vehicle range for $\delta^{15}N\text{-}NO_x$, whereas values at all other sites along the gradient showed mixing between vehicular and biogenic NO_x sources, dependent on distance from the highway. A two end-member mixing model reveals that at the site closest to the road, between 61 and 100% of NO_2 comes from automobile sources. In addition to spatial pattern, $\delta^{15}N\text{-}NO_2$ exhibited a seasonal variation similar to seasonal variations in NO_2 flux (Figure 2.3c). $\delta^{15}N\text{-}NO_2$ was lowest during September at most sites (12, 90, 188 and 460m). During October and November $\delta^{15}N\text{-}NO_2$ increased at all sites. The highest values were in November, which is during the period with the highest NO_2 flux. The lower $\delta^{15}N\text{-}NO_2$ values in August and September reflects the influence of biogenic sources during the growing season. According to

the mixing model, at the site 2m from the road, in August and September, automobile sources accounted for 61-79% of NO_2. In October and November, 93-100% of NO_2 at this site is from automobiles. Despite the seasonal variation, the spatial gradient remained consistent during each sampling month, indicating that mobile NO_2 emissions continually influence the road gradient throughout the study, especially within 12m of the road.

In comparison, δ^{15}N-HNO_3 did not exhibit a defined spatial gradient like the NO_2 isotopes (Figure 2.2d). Isotope values ranged from -1.1 to +3.3‰, which is within the vehicle δ^{15}N-NO_x range; however, individual sites were not significantly different each other (ANOVA, p=0.05). This suggests that measured HNO_3 most likely formed from multiple sources, in addition to vehicle-sourced NO_2. This is likely given the atmospheric lifetime of HNO_3 of several days and the potential for regional transport [*Neuman et al.*, 2006]. Temporal trends in δ^{15}N-HNO_3 were dominated by lower δ^{15}N values at all sites in September relative to other months (Figure 2.3d). However, relative to NO_2, δ^{15}N-HNO_3 values spanned a smaller range and, apart from September values, were relatively constant across the sites during the study period.

2.3.2 Plant tissue isotopic composition

By experimental design, grass nutrient sources were effectively restricted to the potting soil and atmospheric deposition/stomatal uptake. Thus, δ^{15}N values in plant tissue allowed monitoring of plant exposure to atmospheric dry N deposition from automobile and biogenic emissions. We observed pronounced spatial gradients in δ^{15}N values of Bentgrass and Switchgrass (Figure 2.2e and f); however, Bentgrass was a more robust indicator of atmospheric uptake. Bentgrass had

increased $\delta^{15}N$ values close to the road. Bentgrass at the 30m site was significantly different from that at sites at 90, 188 and 460m (ANOVA, p=0.02). The higher $\delta^{15}N$ values in plants near the roadway indicate that these plants were taking up excess N from a higher $\delta^{15}N$ source, in this case automobile pollution. This is in agreement with other studies which have reported increases in plant tissue $\delta^{15}N$ near roadways in comparison with control sites [*Ammann et al.*, 1999; *Pearson et al.*, 2000; *Saurer et al.*, 2004]. Switchgrass $\delta^{15}N$ values also increase near the road, but its peak mean value is at 90 meters from the roadway (Figure 2.2f). Plants at the 12m site were the most variable, but on average had higher $\delta^{15}N$ than the plants at the 460m site. However, the only significant difference between averages at all the sites was 90m and 460m sites (ANOVA, p=0.03). This may indicate that Switchgrass was not receiving N nutrition from atmospheric NO_2; this species might take up more N through the roots or as atmospheric NH_3 or HNO_3.

Temporal trends in spatial patterns of $\delta^{15}N$ also suggest that Bentgrass is a more robust indicator of atmospheric N uptake. Temporally, $\delta^{15}N$-Bentgrass decreased slightly from August until October at all sites (Figure 2.3f). This is not necessarily expected given increasing N flux during those months; however, October marks the end of the plant growing season, slowing/limiting N uptake during this period. In comparison, temporal changes in Switchgrass $\delta^{15}N$ varied by site (Figure 2.3e). At the 12m and 30m sites, $\delta^{15}N$ increased throughout the months of the study. At all other sites $\delta^{15}N$ decreased. Because Switchgrass varied by month without clear trends, atmospheric dry N deposition may be a less important nutrient source. This is further reflected in soil $\delta^{15}N$ for Switchgrass (Figure 2.2l). Soil $\delta^{15}N$ from Switchgrass pots varies most close to the road, with $\delta^{15}N$ values peaking at the 90m site and decreasing with distance from the road. The similarity between Switchgrass tissue and soil $\delta^{15}N$ values suggests

that Switchgrass is primarily receiving N nutrition from the soil. In contrast, $\delta^{15}N$ of Bentgrass soil (Figure 2.2k) shows no clear trends across the gradient and is dissimilar to Bentgrass tissue $\delta^{15}N$. These results indicate that Bentgrass tissue incorporates nitrogen derived from atmospheric sources and thus is a more robust biomonitor for atmospheric N.

Because plant tissue total N and $\delta^{15}N$ values are not necessarily correlated [*Pearson et al.*, 2000], C:N ratios in plant tissue can also be used to evaluate the effects of excess N deposition on plants. For Switchgrass, C:N is lowest closest to the road and increases and becomes more variable with distance from the road (Figure 2.2j). Though not as robust as Switchgrass, Bentgrass followed a similar trend (Figure 2.2i). Bentgrass C:N gradually increases with distance from the road, though no site is significantly different from any other (ANOVA, p=0.05). Seasonal variation can help explain the average C:N values for both grasses. While Switchgrass C:N starts out with similar values in July at all sites, throughout the months of the study, C:N increases at the 188 and 460m site (Figure 2.3g). In August, September and October, C:N ratios at the 12m site were significantly different from those at 460m (ANOVA, p=0.05). Bentgrass exhibited a similar response. Bentgrass C:N was comparable at all sites along the gradient in July (Figure 2.3h); however by August, C:N ratios were higher at the 460m site relative to those closer to the road. The temporal variations observed in Switchgrass and Bentgrass C:N ratios indicate that plants far from the road were the most N limited; as plants used up the nutrients in the potting soil, the C:N ratios increased throughout the months of the study. In contrast, the plants closer to the road received a continuous supply of N deposition, which contributed to their N nutrition and resulted in lower C:N ratios. This mechanism can explain why species compositions in plant communities near roadways often have a greater proportion of N-tolerant plants [*Angold*, 1997; *Bignal et al.*, 2007].

C isotopes provide another way to examine the impacts of fossil fuel emissions on plant tissue along the road gradient. Because plants take up CO_2 from the atmosphere during photosynthesis, C isotopes in plant tissue can indicate the sources of CO_2 to which the plants were exposed. The two sources of CO_2 in this system are background atmospheric CO_2, characterized by $\delta^{13}C$ of -8‰ [*Keeling et al.*, 1989], and fossil fuel CO_2 from automobiles, with a $\delta^{13}C$ value of around -27‰ [*Bush et al.*, 2007; *Clark-Thorne and Yapp*, 2003]. It follows that plants that are impacted by fossil fuel emissions would have lower $\delta^{13}C$ values than plants that are not. For Bentgrass, C isotopes were more positive farther from the road (Figure 2.2g). However, this relationship was not significant (ANOVA, p=0.05) and varied by month. In July and August, Bentgrass-$\delta^{13}C$ values were approximately the same across the entire gradient. In September and October, the 460m site had $\delta^{13}C$ values approximately 1‰ higher than the 30m site, indicating that plants at the sites closer to the road may have been affected by fossil fuel emissions. C isotopes for Switchgrass followed a more defined trend (Figure 2.2h). $\delta^{13}C$ of Switchgrass at the 12m site were significantly lower than the 90 and 188m site (ANOVA, p=0.05). In each month, the 460m site had values approximately 1‰ higher than the 12m site. This is in agreement with another road gradient study in which $\delta^{13}C$ values in plant tissue 1m from a roadway were lower than 50m from the road [*Lichtfouse et al.*, 2002]. Because the spatial scale of this study was small and CO_2 is well mixed in the atmosphere, we would expect the variation in $\delta^{13}C$ values along the road gradient to be limited (<1‰); larger variations in $\delta^{13}C$ values (~5‰) were measured in a study of $\delta^{13}C$ values in plant tissue along a longer urban to rural gradient [*Lichtfouse et al.*, 2002].

2.3.3 Implications

Automobile emissions can contribute up to four times more N deposition to near-road environments than regional background deposition. However, near-road deposition fluxes are not necessarily accounted for by sites included in existing national monitoring networks. These sites measure N deposition in locations far from roadways and they also do not measure NO_2, one of the primary pollutants from automobiles. This underestimation of N deposition can be especially important in urban areas, where there is a high density of roadways and increased vehicular traffic. In order to assess the amount of total atmospheric N deposition reaching the landscape, establish accurate N budgets, and develop useful mitigation strategies for atmospheric N pollution, monitoring in urban areas and near roadways must occur.

Furthermore, near-road hotspots of increased N deposition have implications for roadway ecosystems. Roadside water diversion infrastructure can channel excess dry N deposition directly into sewers and surface water, where increases in nitrate concentrations in waters can lead to acidification and eutrophication. In addition, excess N can have negative impacts on near-road vegetation, leading to increases in N tolerant species near roads and declining vegetation health. However, the increase in plant uptake of N near the roadway may indicate that roadside plants could be used to mitigate the effects of excess N, though further research is needed to verify this.

3.0 ISOTOPIC INVESTIGATION OF ANTHROPOGENIC SOURCES OF CARBON AND NITROGEN TO VEGETATION ALONG TWO URBAN TO RURAL GRADIENTS

3.1 INTRODUCTION

Excess reactive nitrogen additions to the environment can have widespread detrimental effects on ecosystem health. For example, increased fluxes of N to terrestrial and aquatic systems can cause acidification and mobilization of metals and base cations [*Rabalais*, 2002]. In addition, N loading in aquatic systems can cause eutrophication and subsequent dead zones in major water bodies [*Howarth et al.*, 1996; *Nixon*, 1995]. In the absence of other sources, ecosystem inputs of reactive N are roughly equal to outputs of N_2 from denitrification, which balances nitrogen cycling. However, human activities alter the N cycle through inputs of reactive N from fossil fuel combustion and fertilizer application. Currently, the addition of anthropogenic reactive nitrogen to ecosystems exceeds that from natural sources [*Galloway et al.*, 2004].

Atmospheric N deposition is a major source of anthropogenic N. Emissions from fossil fuel burning produce nitrogen oxides (NO and NO_2), which further oxidize to form HNO_3. These compounds are removed from the atmospheric in either wet (dissolved in precipitation) or dry (aerosols and particulates) deposition. While wet deposition makes up the majority of total N deposition in the eastern U.S., dry deposition accounts for 20-50% [*Butler et al.*, 2005], and thus can be a significant source of N to ecosystems.

Atmospheric N deposition in urban areas is poorly characterized because N monitoring is primarily done at remote locations. For example, national monitoring networks, such as the National Atmospheric Deposition Program- National Trends Network and the Clean Air Status and Trends Network (CASTNET), intentionally locate sites in rural areas to capture regional background levels of deposition. This may potentially cause an underestimation of the amount of atmospheric N reaching the land surface, as it does not take in to account hotspots of N deposition near area sources of pollution, such as roadways and urban areas. Therefore, in order to more accurately characterize the amounts of total N deposition reaching the landscape, it is necessary to examine N deposition in urban areas.

Isotopic studies can give insight into the sources of local N deposition, allowing us to separate natural from anthropogenic-sourced N. The major sources of anthropogenic and biogenic NO_x have different $\delta^{15}N$ values (reported in parts per thousand compared to atmospheric N_2; See Table 1.1.). Vehicular sources have reported $\delta^{15}N$-NO_x of +3.7 to +9‰ [*Ammann et al.*, 1999; *Freyer*, 1978; *Heaton*, 1990; *Moore*, 1977] (more negative values, -13 to -2‰ [*Heaton*, 1990], have been reported, but these values were from exhaust of idling vehicles). Power plant NO_x emissions have $\delta^{15}N$ values of +6 to +20‰ [*Felix et al.*, submitted; *Heaton*, 1990]. Biogenic emissions have much lower N isotopic values of -19 to -49‰ [*Li and Wang*, 2008]. While N isotope studies of wet deposition have been conducted across local and regional scales [*Elliott et al.*, 2007; *Hastings et al.*, 2003; *Hastings et al.*, 2004; *Kendall and McDonnell*, 1998], there are fewer isotopic studies on dry N deposition. A study by Freyer [1993] examined $\delta^{15}N$ of gaseous NO_2 in a small German city, while a more recent study by Elliott, et al. [2009] investigated patterns in $\delta^{15}N$ of HNO_3 and particulate NO_3- across rural sites in New York, Pennsylvania and Ohio.

This study characterizes the amount and sources of dry N deposition along two urban to rural gradients. We used passive samplers to collect dry N deposition for analysis of both concentration and stable isotopes of nitrogen. This method provides an easy and inexpensive way to monitor N deposition across large spatial gradients for extended time periods.

In addition, we deployed grasses as biomonitors to assess the influence of excess dry N deposition in urban areas on N content and isotopic composition of plant tissue. While plants assimilate most nitrogen through the roots, atmospheric NO_x, HNO_3 and NH_3 taken up through the leaves can also be an important nutrient source [*Garten*, 1993; *Padgett et al.*, 2009; *Thoene et al.*, 1991; *Wellburn*, 1990]. This is evidenced by several studies that document that $\delta^{15}N$ composition of plant tissue reflects $\delta^{15}N$ of atmospheric NO_x [*Ammann et al.*, 1999; *Pearson et al.*, 2000; *Saurer et al.*, 2004]. This study couples passive sampling of dry N deposition and plant biomonitors to delineate the sources and magnitude of N deposition to urban and rural areas and associated influence on local vegetation.

Analysis of $\delta^{13}C$ of plant tissue provides another way to examine the impacts of fossil fuel emissions on urban vegetation. Several studies document a "dome" of CO_2 concentrations around urban areas, caused by increased fossil fuel emissions in urban centers [*Idso et al.*, 2001; *Pataki et al.*, 2007; *Ziska et al.*, 2003]. The major sources of atmospheric CO_2 are global background CO_2, which has a $\delta^{13}C$ isotopic composition of -8‰ [*Keeling et al.*, 1989], and fossil fuel emission CO_2, which has a $\delta^{13}C$ value of -27‰ [*Bush et al.*, 2007; *Clark-Thorne and Yapp*, 2003]. Therefore, environments with major CO_2 inputs from fossil fuel combustion have lower $\delta^{13}C$-CO_2 values than the global average, due to the mixing of anthropogenic CO_2 with background atmospheric CO_2 [*Pataki et al.*, 2003]. Furthermore, the isotopic signature of atmospheric CO_2 can be incorporated into plant tissue through photosynthesis. Previous studies

have shown that the $\delta^{13}C$ composition of plant tissue reflects the $\delta^{13}C$ of ambient CO_2 [*Farquhar et al.*, 1989; *Lichtfouse et al.*, 2002; *Pepin and Körner*, 2002]. It follows that because urban areas have elevated CO_2 concentrations from fossil fuel combustion, the $\delta^{13}C$ values of plant tissue in urban areas should be lower than that of rural areas. In this study, we used plant biomonitors to test that hypothesis.

3.2 METHODS

3.2.1 Sites

Research sites consisted of two urban to rural gradients, one in Baltimore, MD and the other in Pittsburgh, PA (USA). Each gradient contained three sampling locales: one urban, one suburban and one rural. The Maryland gradient spanned approximately 209 kilometers from downtown Baltimore to the New Jersey Pine Barrens (Figure 3.1). More specifically, the urban site was located at the Maryland Science Center in downtown Baltimore, near the city center. This site is characterized by a high street (and thereby traffic) density and many large buildings. Suburban samples were collected from a U.S. Forest Service eddy flux tower in Cub Hill, MD. This site is surrounded by medium density residential land use. Rural sampling was conducted at the Rutgers University Pinelands Research Center in the U.S. Forest Service Silas Little Experimental Forest in New Lisbon, New Jersey. This site is located in a wooded area with very few houses and low traffic density.

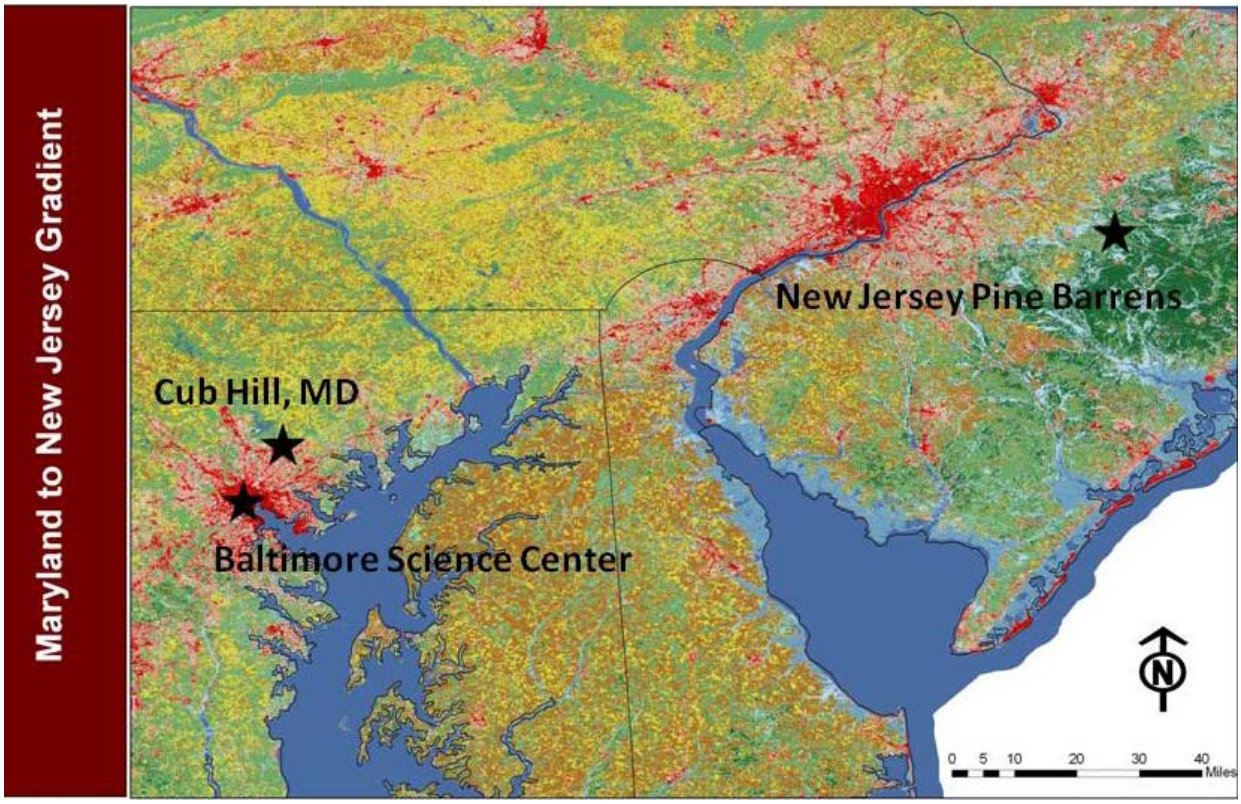

Figure 3.1: Baltimore gradient map. Sites are shown on a land use/land cover map. Red indicates urban areas, pink is suburban, yellow is agricultural and green is forested.

The Pittsburgh urban to rural gradient spanned approximately 80 kilometers from Pittsburgh, PA to Rector, PA (Figure 3.2). Urban samples were collected in Hazelwood, a formerly industrial and presently residential neighborhood located about four miles from downtown Pittsburgh. This site is within the city limits and is characterized by high street and housing density. Suburban samples were acquired from the Westmoreland Conservation District in Greensburg, PA, a small city ~35 miles east of Pittsburgh. Samplers were located near a strip mall and several housing developments. Rural sampling was completed at the Carnegie Museum of Natural History Powdermill Nature Reserve in Rector, PA. This site is surrounded by low-density housing and forest.

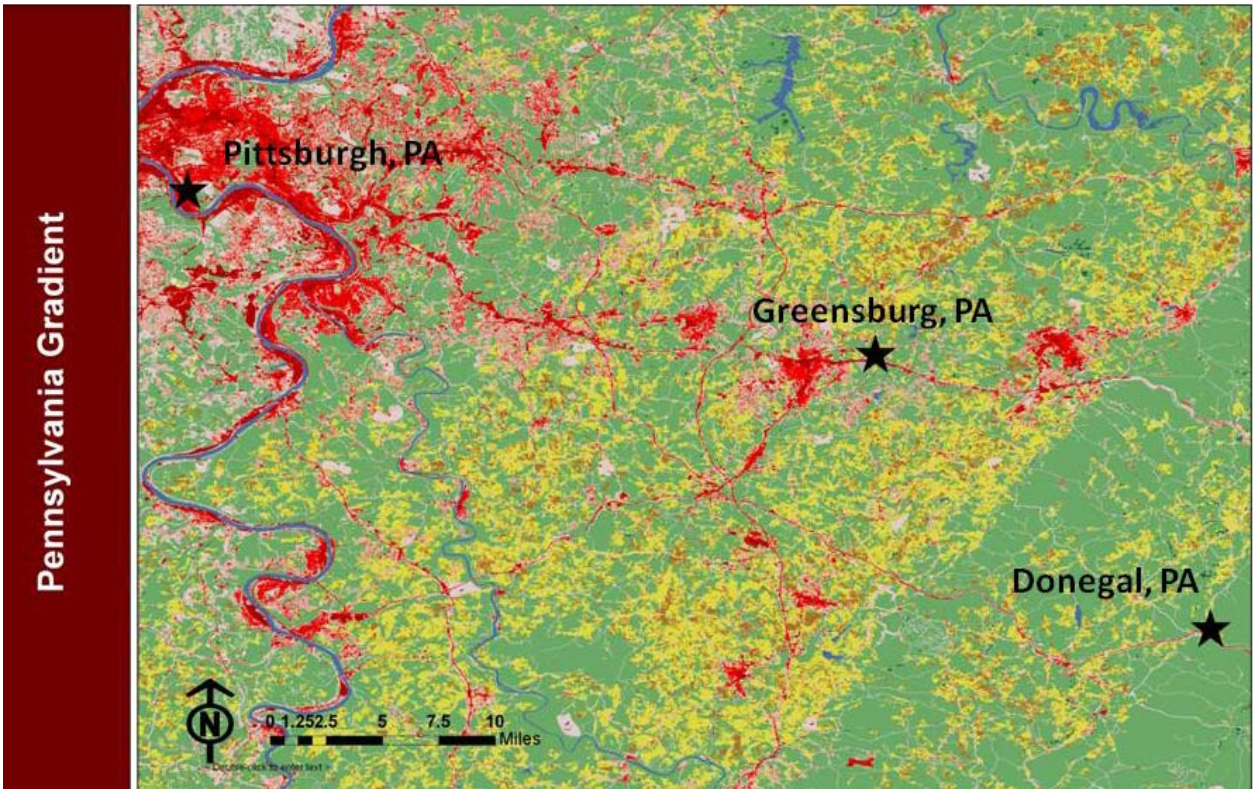

Figure 3.2: Pittsburgh gradient map. Sites are shown on a land use/land cover map. Red indicates urban areas, pink is suburban, yellow is agricultural and green is forested.

3.2.2 Plants biomonitors

All experimental plants were grown from seed in Pittsburgh in an identical potting mixture. Five replicate pots of *Agrostis perennans* (Autumn Bentgrass) and *Panicum virgatum* (Switchgrass) were set in holes in the ground at each site along the gradients. Approximately fifty individual plants were growing in each pot. The plastic pots were doubled to prevent water loss and to isolate the roots from native soils. This ensured that the plants effectively only received nutrients from the potting soil and atmospheric sources. Plants were sampled for isotopic analysis prior to field deployment to measure similarity in initial isotopic compositions. During field deployment, plants and soil were sampled once a month for four months, July-October, 2008. Leaf samples

were cut with scissors, washed with Milli-Q water and placed in individual bags. In addition, soil was sampled from each pot every month concurrent with plant sampling. Approximately 100 grams of soil were spooned out of the pots from a depth of 2-5 centimeters and placed in individual bags. Both plants and soil were stored on ice for transport to the laboratory and then frozen to prevent tissue breakdown. For analysis samples were freeze dried, ground with a commercial coffee grinder and with a mortar and pestle and loaded into tin capsules for isotopic analysis of C and N. The samples were combusted in a Eurovector high temperature Elemental Analyzer connected to a GV Instruments Isoprime (now Elementar Americas) Continuous Flow Isotope Ratio Mass Spectrometer (CF-IRMS) to determine both carbon and nitrogen concentration and isotopic composition. For all analyses in this study, data for July is not shown. As the plants acquired biomass, carbon and nitrogen isotopes changed as juvenile plants matured. In July, the isotope ratios measured in the plants were a mix between the seedlings started in June and the full grown plants from August and later; therefore our data analyses only considers mature plant tissue.

3.2.3 Gaseous sampling

Two forms of dry nitrogen deposition, NO_2 and HNO_3, were collected with passive diffusion samplers at each site. Samplers for NO_2 were purchased from Ogawa, USA, and samplers for HNO_3 were similar to the USDA Forest Service design described by Bytnerowicz *et al.* [2005]. The samplers collect atmospheric species on a chemically reactive filter pad. Each gas required a different filter. For NO_2, we used pre-coated filters purchased from Ogawa, USA. HNO_3 was collected using a 47mm nylon filter (Pall Corporation). These samplers are an effective and

inexpensive method for monitoring dry deposition [*Bytnerowicz et al.*, 2005] and isotopic composition [*Elliott et al.*, 2009]. Samplers were deployed for one month intervals, allowing adequate material for analysis to collect on the filters. Each sampler holds two filters, which ensures that sufficient material is collected each month to perform both concentration measurements and isotopic analysis of each species. Each month the filters were changed in the field at the same time the grasses and soils were sampled. In addition, we used field and laboratory blanks to determine background levels of deposition on the filters prior to deployment.

For concentration measurements of NO_2 and HNO_3, we eluted each filter with 5mL of Milli-Q water to produce nitrate (NO_3-) and nitrite (NO_2-). The eluant was injected into a Dionex ICS2000 Ion Chromatograph. For isotopic analysis of NO_2 and HNO_3 we eluted the second filter of each sample in 5mL of Milli-Q water. We then used the bacterial denitrification method to convert the eluted NO_2- and NO_3- into 10 nanomoles of N_2O gas [*Casciotti et al.*, 2002; *Sigman et al.*, 2001]. The resulting gas was introduced into a GV Instruments Isoprime CF-IRMS. Samples with eluant concentrations of less than 0.23 mg/L were not run for isotopic analysis due to insufficient nitrogen mass. For HNO_3, this included the Baltimore rural site in October. For NO_2, this included the Baltimore rural site in August and September, the Baltimore suburban site in July, and the Pittsburgh rural site in August.

In order to calculate a flux in kg ha^{-1} yr^{-1} from the concentration data, we used the method described by [*Golden et al.*, 2008] in which:

$$F = (C \times v) / (a \times d)$$

where F is flux, C is the concentration measured in filter eluant, v is elution volume, a is the effective filter area and d is the number of days the filter was exposed. These calculations yield

units of kg ha^{-1} yr^{-1}, which is a standard method of reporting N flux. However, the filters represent *monthly* average concentrations. Therefore, the kg ha^{-1} yr^{-1} value for each month is the amount of N flux in kg ha^{-1} yr^{-1} that would occur for the whole year if the concentrations for that month were consistent throughout the year.

3.3 RESULTS

3.3.1 Nitrogen flux

Average total N (HNO_3 + NO_2) flux for the Baltimore gradient was highest at the urban site and lowest at the rural site, 1.26 and 0.84 kg ha^{-1} yr^{-1}, respectively (Figure 3.3a). Each site differed in the proportion of average HNO_3 to NO_2 deposition. At the rural site HNO_3 flux was higher than NO_2 flux, but at the suburban and urban sites NO_2 flux was higher. Fluxes also exhibited monthly differences (Figure 3.3c). For example, HNO_3 deposition peaked at the rural and suburban sites in September. In addition, NO_2 deposition increased during the colder months (October and November) at all sites.

Along the Pittsburgh gradient (Figure 3.3b), average total N (HNO_3 + NO_2) flux was highest at the urban site (1.70 kg ha^{-1} yr^{-1}), whereas the suburban site had the lowest total N flux (0.72 kg ha^{-1} yr^{-1}). The rural sampling location yielded intermediate values, averaging 0.93 kg ha^{-1} yr^{-1}. At each site, NO_2 was the highest contributor to total N flux.

N flux at the Pittsburgh gradient also varied seasonally (Figure 3.3d). HNO_3 was highest in July, relatively low for August and September, and then increased slightly in October. Like the Baltimore gradient, NO_2 at the Pittsburgh gradient increased throughout the course of the

study, with the highest NO_2 fluxes occurring in November at all sites. This is in agreement with other studies which have documented increases in NO_2 concentrations in winter months [*Atkins and Lee*, 1995; *Kirby et al.*, 1998].

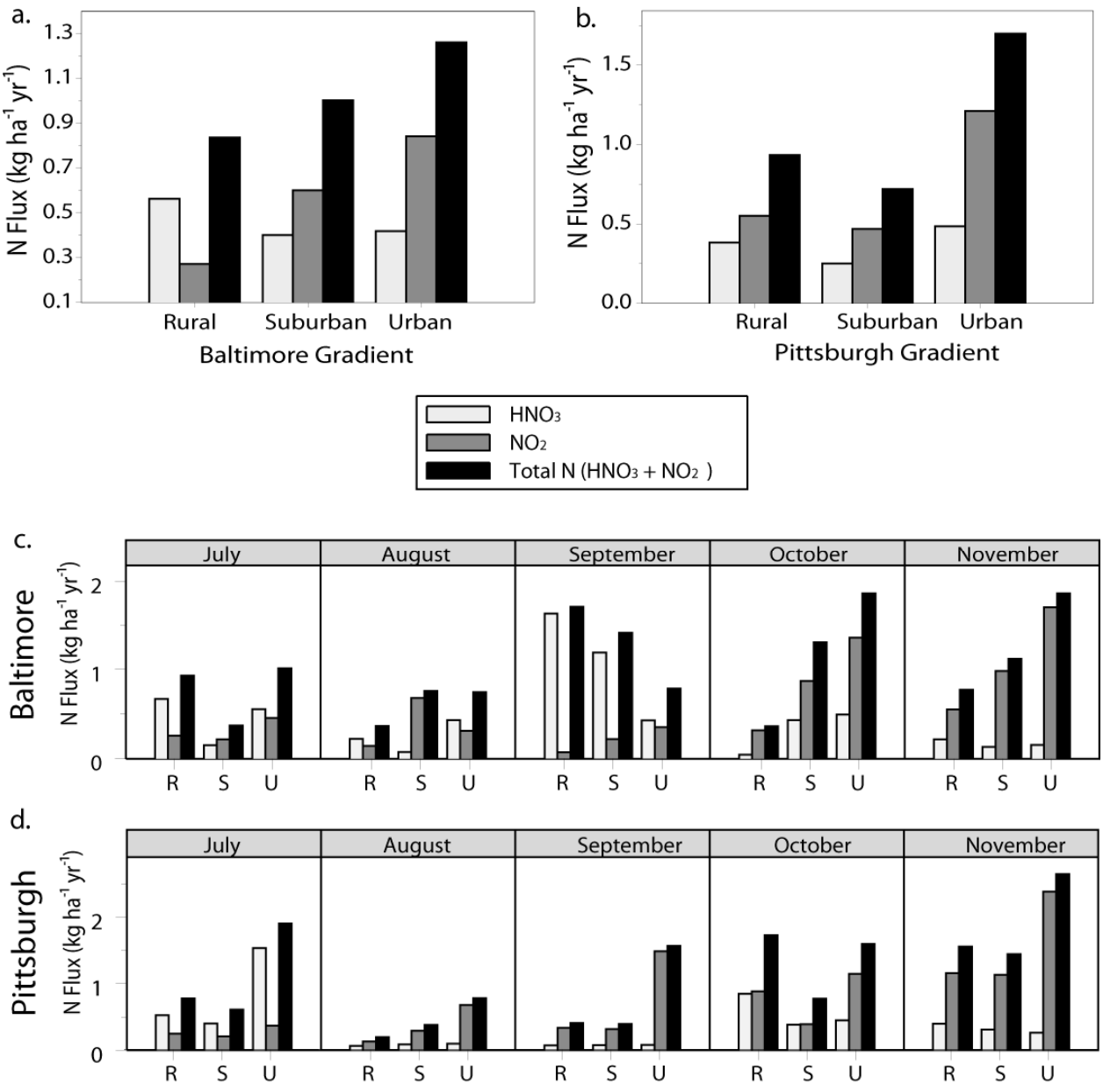

Figure 3.3: Nitrogen Flux. HNO_3, NO_2 and total N (HNO_3 + NO_2) flux estimates (kg ha^{-1} yr^{-1}) for the Baltimore and Pittsburgh gradients. Boxes a and b represent the averages for all months of the study. Boxes c and d are individual monthly values for the rural, suburban and urban sites (R, S, U, respectively).

3.3.2 Nitrogen deposition isotopes

$\delta^{15}N\text{-}HNO_3$ at the Baltimore gradient had the highest average values at the suburban site (Figure 3.4a). The suburban site was significantly different than the urban site (ANOVA, p=0.05, n=14). $\delta^{15}N\text{-}HNO_3$ did not exhibit consistent seasonal effects along the gradient. For example, in August $\delta^{15}N\text{-}HNO_3$ values at the suburban and rural sites were the lowest (Figure 3.4c), while all other months were ~1 to 2‰ higher. The urban site did exhibit seasonality; $\delta^{15}N\text{-}HNO_3$ values gradually increased during each month of the study.

$\delta^{15}N\text{-}HNO_3$ values for the Pittsburgh site (Figure 3.4b) had the highest mean value at the urban site; however, mean values at the three sites were not significantly different (ANOVA, p=0.05, n=15). The Pittsburgh gradient HNO_3 isotopes exhibited seasonal variation; lowest values for all three sites occurred in September (Figure 3.4d). Furthermore, in October and November, $\delta^{15}N\text{-}HNO_3$ values were lowest at the rural site and highest at the urban site. $\delta^{15}N\text{-}HNO_3$ did not correspond with HNO_3 flux at the Pittsburgh and Baltimore more gradients.

Average $\delta^{15}N\text{-}NO_2$ values along the Baltimore gradient were similar between all the sites; however these values encompassed a large range (-25 to -7‰) (Figure 3.5a). No significant difference in mean values was observed between any of the sites (ANOVA, p=0.05, n=12). However, there was a marked seasonal pattern in $\delta^{15}N\text{-}NO_2$; in October and November values at all three sites increased by 10 to 15‰, with the greatest increase at the urban sites (Figure 3.5c). The increase in $\delta^{15}N\text{-}NO_2$ values in October and November also corresponds with the increase in NO_2 flux during these months.

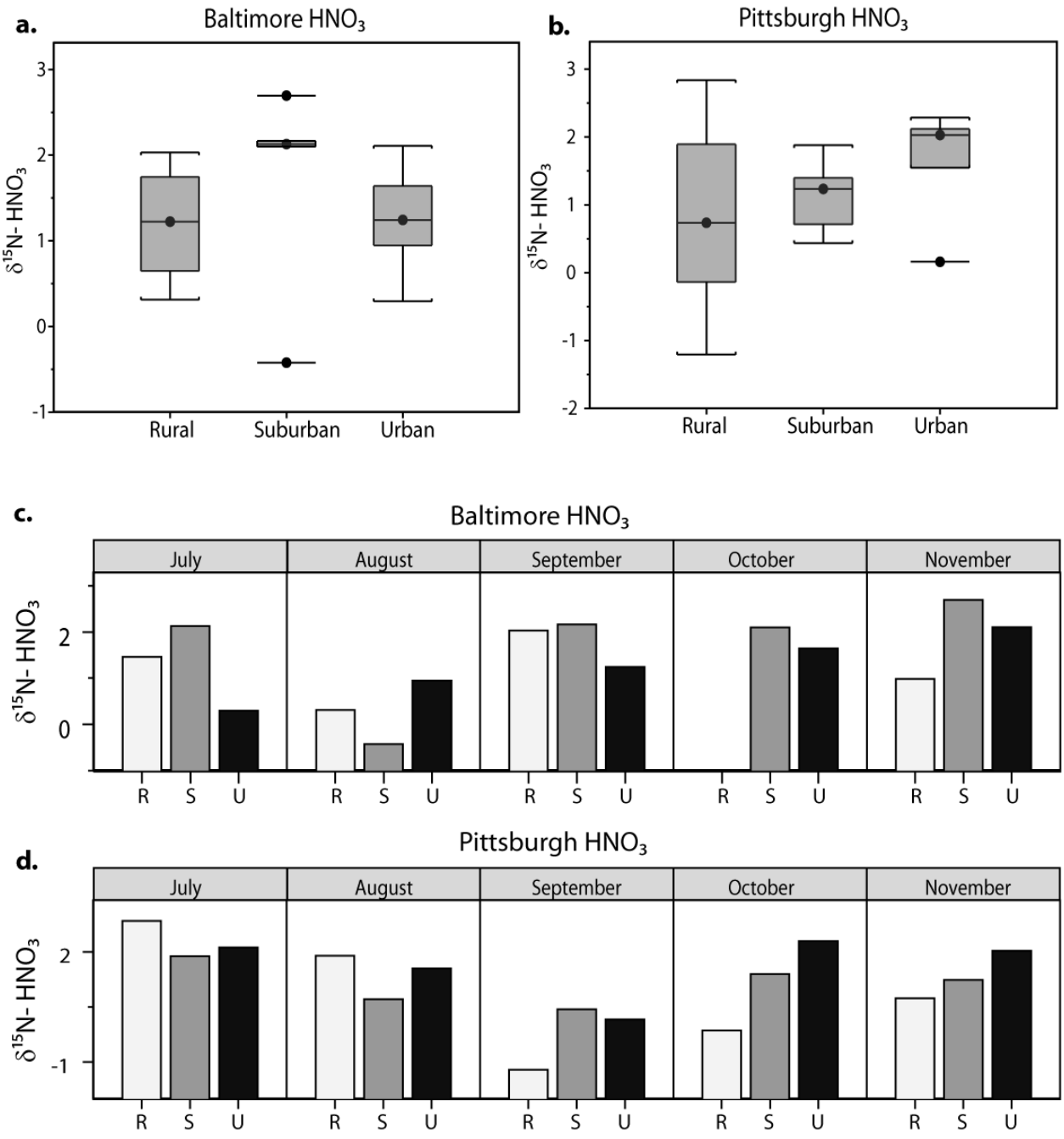

Figure 3.4 HNO_3 Isotopes along the Baltimore and Pittsburgh gradients. Plots a and b are box and whisker plots, in which the box represents the upper and lower quartile and the whiskers represent the minimum and maximum data point. The center line in the box is the median value. Outliers are shown as black dots with lines through them. Plots c and d are monthly values for $\delta^{15}N$-HNO_3 for the rural, suburban and urban sites (R,S,U, respectively).

At the Pittsburgh gradient, the urban site had the highest mean $\delta^{15}N$-NO_2 values, while the suburban site had the lowest mean values (Figure 3.5b). These two sites were significantly different (ANOVA, p=0.01, n=14), with a 17‰ difference in mean values. In each month, the urban site had the highest $\delta^{15}N$-NO_2 values and the suburban site had the lowest values. $\delta^{15}N$-NO_2 values in the Pittsburgh gradient also showed seasonal variations (Figure 3.5d); values at all sites increased in October and were highest in November, corresponding with increases in NO_2 flux.

3.3.3 Plant tissue nitrogen isotopes

$\delta^{15}N$-Bentgrass values showed different patterns in the two urban to rural gradients (Figure 3.6). Bentgrass at the Baltimore gradient had the lowest mean $\delta^{15}N$ values at the suburban site and highest mean $\delta^{15}N$ values at the urban site. Means for the urban and rural site were only 0.1‰ apart, while the mean for the suburban site was ~0.5‰ lower. None of the sites were significantly different from each other (ANOVA, p=0.05, n=40). $\delta^{15}N$-Bentgrass along the Pittsburgh gradient showed the opposite trend. $\delta^{15}N$ values were lowest at the urban site and highest at the suburban site. The average $\delta^{15}N$-Bentgrass values at the suburban and rural sites were significantly different from the urban site (ANOVA,p=0.03,n=45).

Across the Baltimore gradient, the urban site had the highest $\delta^{15}N$-Switchgrass values and the suburban site had the lowest values. All three sites were significantly different from each other (ANOVA, p=0.01, n=45). Along the Pittsburgh gradient, the rural site had some of the highest $\delta^{15}N$-Switchgrass values, but had the lowest median value. The suburban site had the highest mean $\delta^{15}N$ value. The suburban site $\delta^{15}N$ value of Switchgrass was significantly

different from the rural site (ANOVA, p=0.05, n=44), but had similar values for Switchgrass from the urban site.

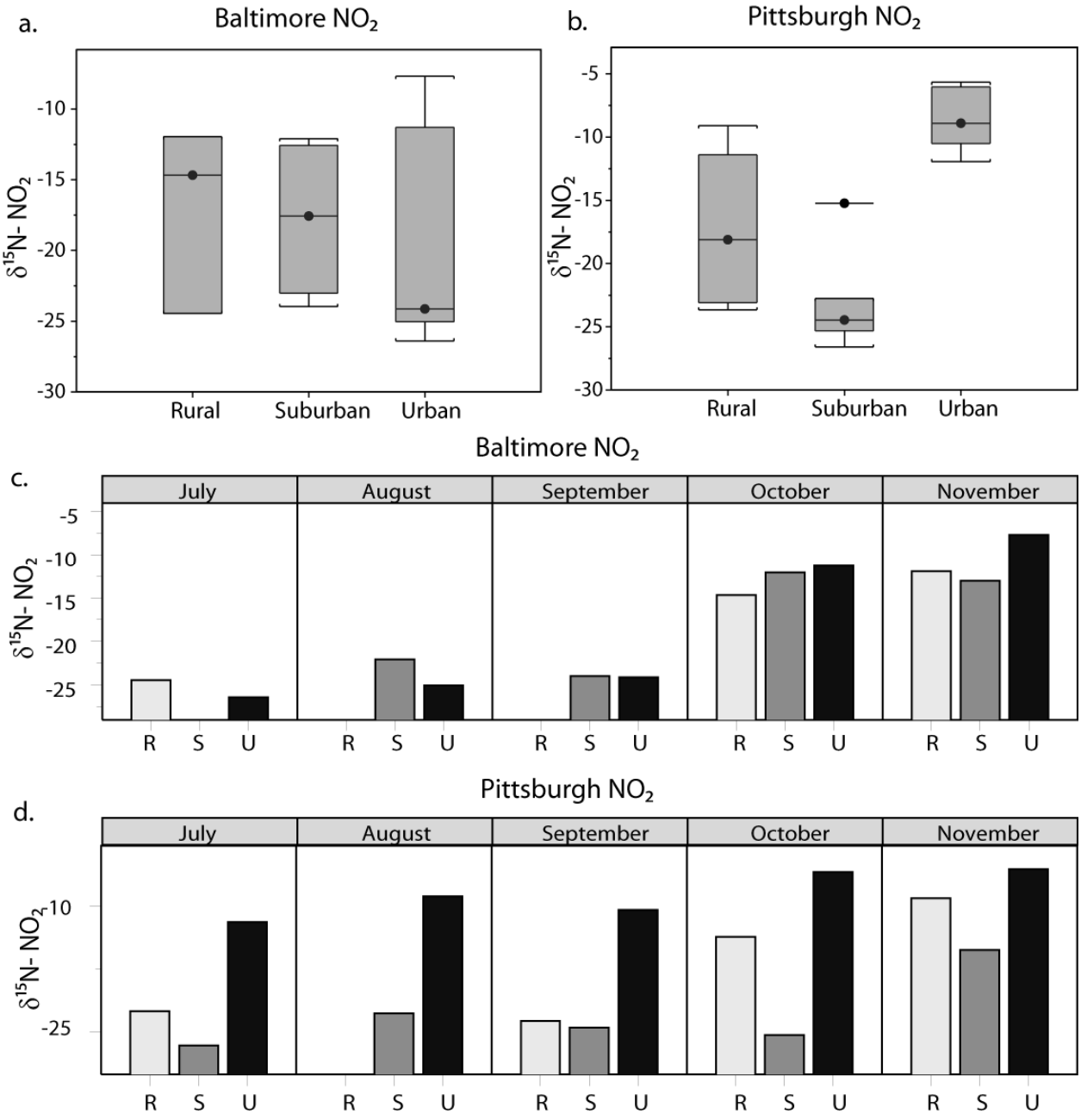

Figure 3.5: NO_2 Isotopes for the Baltimore and Pittsburgh gradients. Plots a and b are box and whisker plots, in which the box represents the upper and lower quartile and the whiskers represent the minimum and maximum data point. The center line in the box is the median value. Outliers are shown as black dots with lines through them. Plots c and d are individual monthly values by rural, suburban and urban site (R,S,U, respectively).

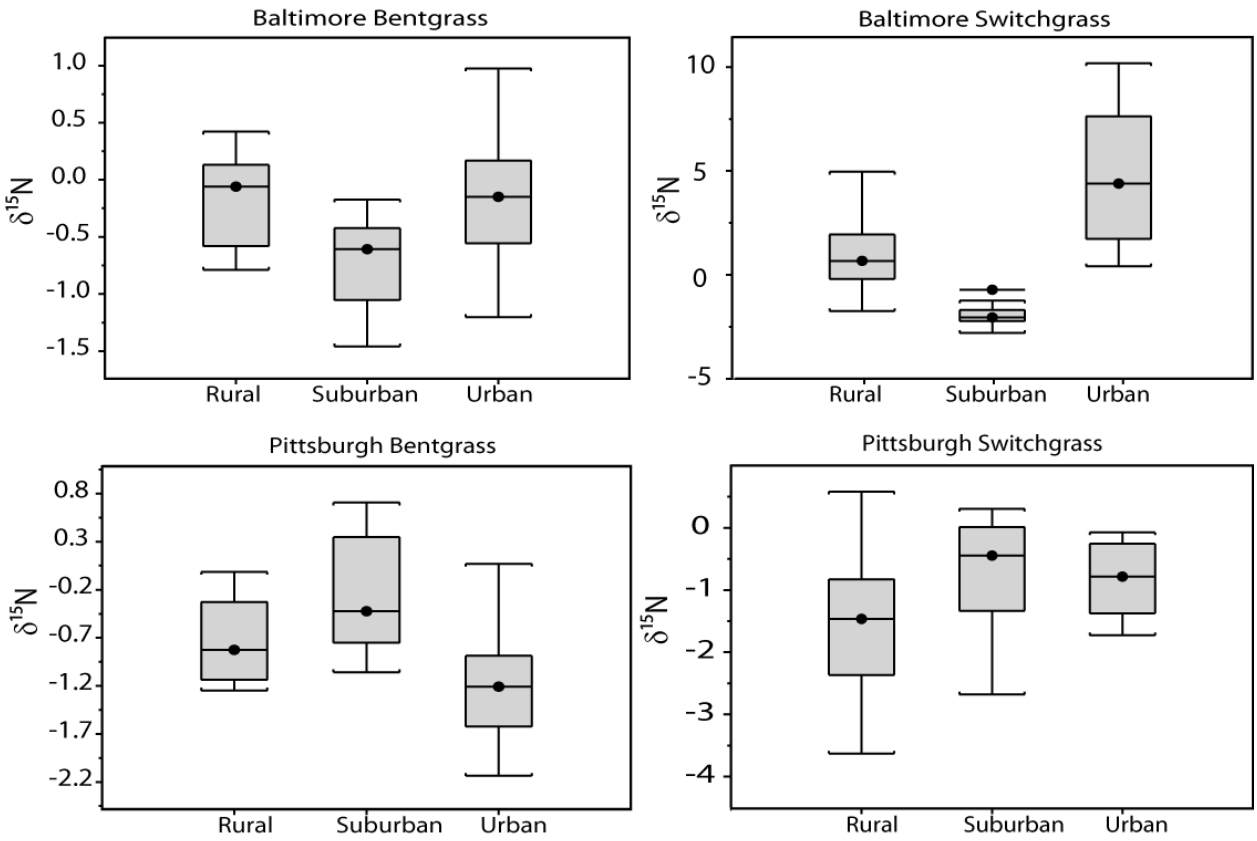

Figure 3.6: Plant Tissue Nitrogen Isotopes for Pittsburgh and Baltimore Bentgrass and Switchgrass. Plots are box and whisker plots, in which the box represents the upper and lower quartile and the whiskers represent the minimum and maximum data point. The center line in the box is the median value. Outliers are shown as black dots with lines through them.
δ^{15}N-Switchgrass also exhibited different patterns at both gradients (Figure 3.6).

3.3.4 Plant tissue carbon isotopes

For Bentgrass, carbon isotopic values in the Baltimore and Pittsburgh gradients were quite different (Figure 3.7). In Baltimore, Bentgrass δ^{13}C values had the largest range in values at the urban site. Mean δ^{13}C-Bentgrass values were highest at the suburban site and lowest at the rural site. None of the sites were significantly different (ANOVA, p=0.05, n=45). Bentgrass at the

Pittsburgh gradient showed a different trend; at the urban site, δ^{13}C-Bentgrass values were lowest, while the rural site had some of the highest values. δ^{13}C-Bentgrass values at the rural and suburban sites were significantly different from the urban site (though not significantly different from each other) (ANOVA, p=0.01, n=45).

Along the Baltimore gradient, δ^{13}C-Switchgrass was lowest at the urban site, while the suburban and rural sites had similar values (Figure 3.7). Both the rural and suburban sites were significantly different from the urban site (ANOVA, p=0.01, n=40). δ^{13}C-Switchgrass along the Pittsburgh gradient was lowest at the urban site and highest at the rural site. All three sites were significantly different from each other (ANOVA, p=0.01, n=44), and thus exhibited the strongest δ^{13}C gradient of both types of grasses and both urban to rural gradients.

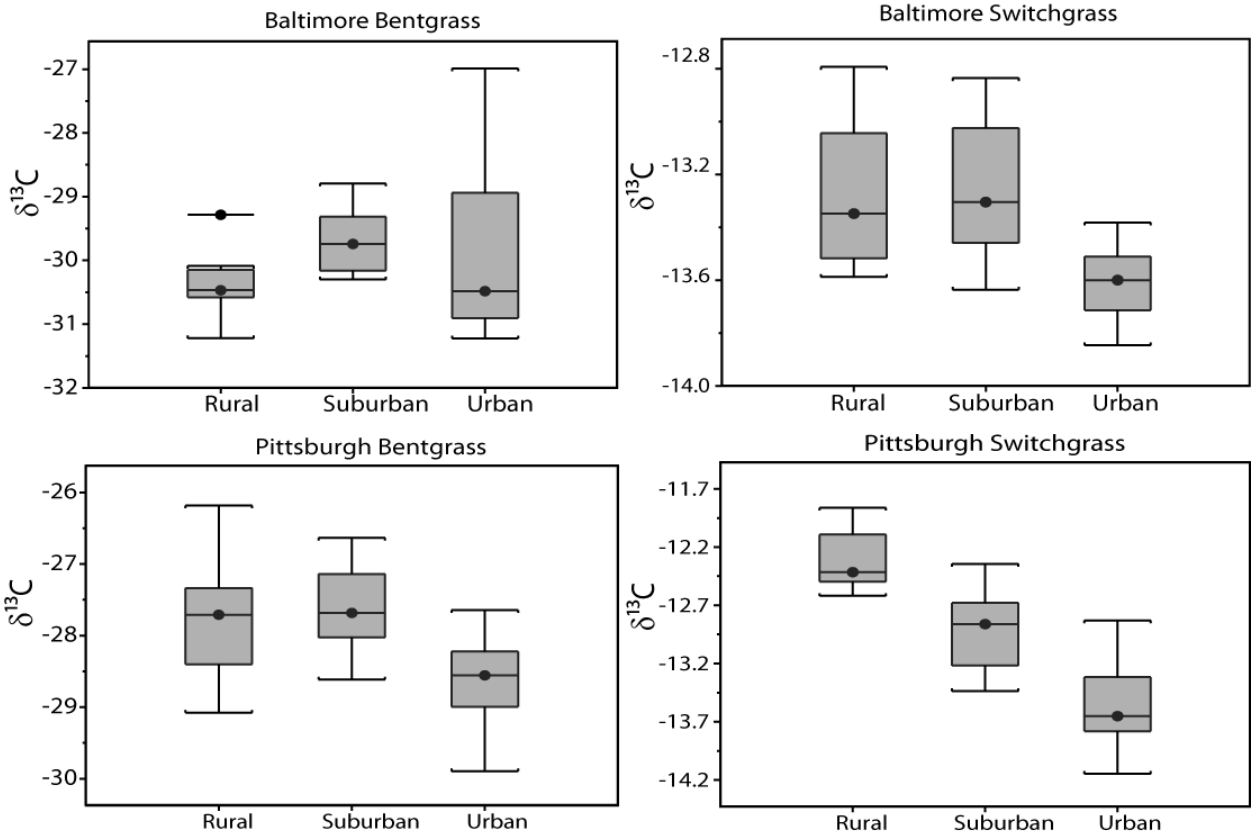

Figure 3.7: Plant tissue carbon isotopes for Pittsburgh and Baltimore Bentgrass and Switchgrass. Plots are box and whisker plots, in which the box represents the upper and lower quartile and the

whiskers represent the minimum and maximum data point. The center line in the box is the median value. Outliers are shown as black dots with lines through them.

3.3.5 Plant tissue nitrogen vs. carbon isotope

It is also important to compare $\delta^{15}N$ against $\delta^{13}C$ in the plant biomonitors (Figure 3.8). We expected rural sites should plot to the upper left of the graph, with more positive $\delta^{13}C$ and more negative $\delta^{15}N$ values, and urban points should plot closer to the lower right of the graph, with more negative $\delta^{13}C$ and more positive $\delta^{15}N$ values (Figure 3.8).

Bentgrass plots from both gradients did not plot as expected (Figure 3.8). The Baltimore Bentgrass urban points plotted toward the bottom right, except for the points from August, which had much higher $\delta^{13}C$ values. Suburban points plotted to the upper left, and rural points plotted in between the urban and suburban. The Pittsburgh Bentgrass plotted with the suburban and rural clusters on top of each other, and the urban points to the bottom left.

Baltimore Switchgrass urban points plotted in the bottom right, as expected, while the suburban and rural points plotted next to each other in the top left (Figure 3.8). Pittsburgh Switchgrass plotted with the urban site in the bottom right, the rural site in the top left, and the suburban site in between.

3.3.6 Plant tissue C to N ratios

C:N ratios in plant tissue can also be used to evaluate the effects of excess N deposition on plants. Baltimore gradient Bentgrass had similar C:N at the rural and urban site, while the suburban site had higher C:N (Figure 3.9). The suburban and urban sites were significantly different (ANOVA, $p=0.05$). Pittsburgh gradient Bentgrass showed a clear gradient in C:N, with

lowest values at the urban site and highest values at the rural site. All three sites were significantly different (ANOVA, p=0.01). At both locations, C:N showed seasonal variation. Values were lower throughout the growing season and were higher in October, at the end of the growing season.

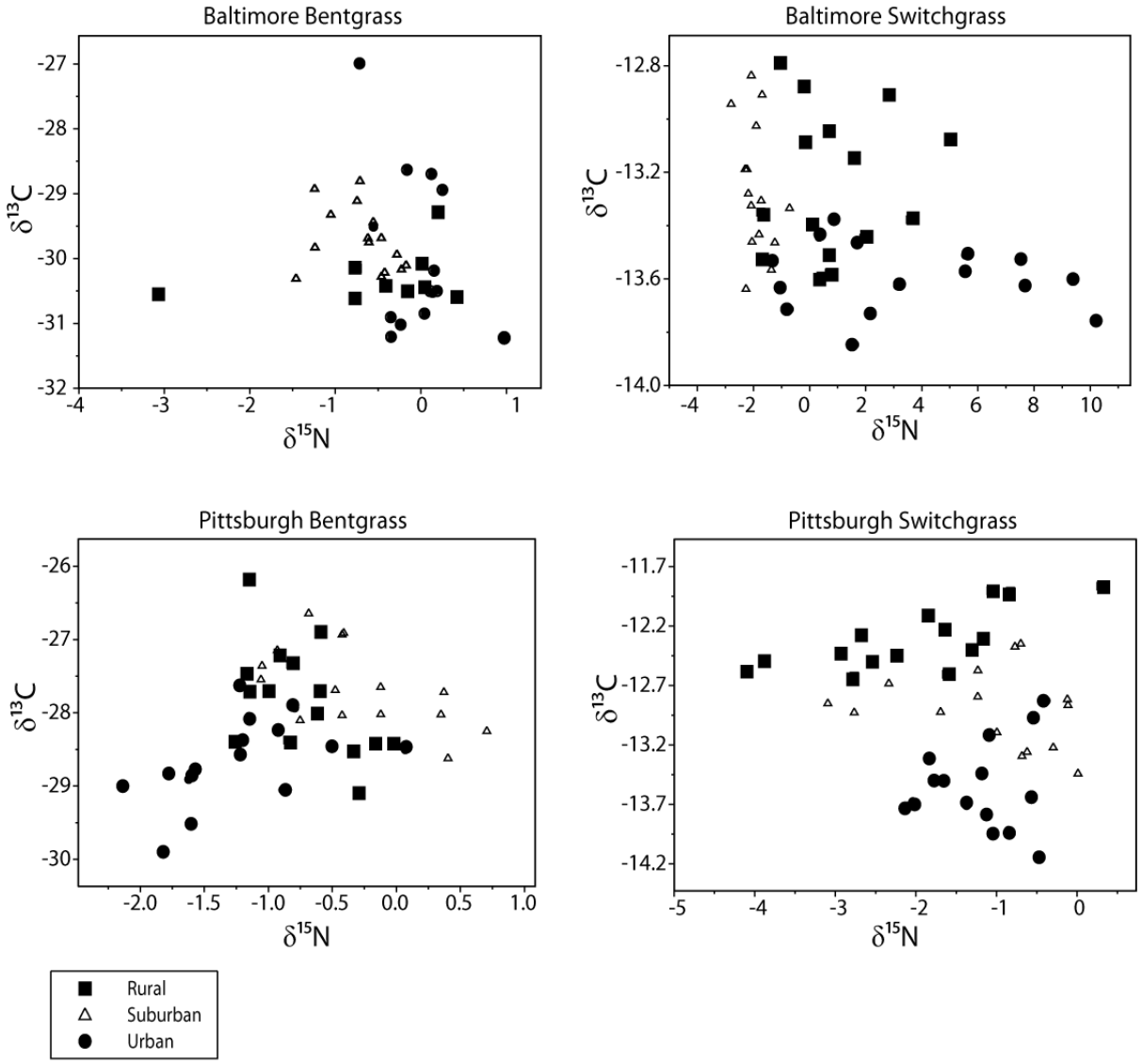

Figure 3.8: Nitrogen and carbon isotope plots for plant biomonitors. Urban sites are marked with closed circles, suburban sites are open triangles and rural sites are closed squares.

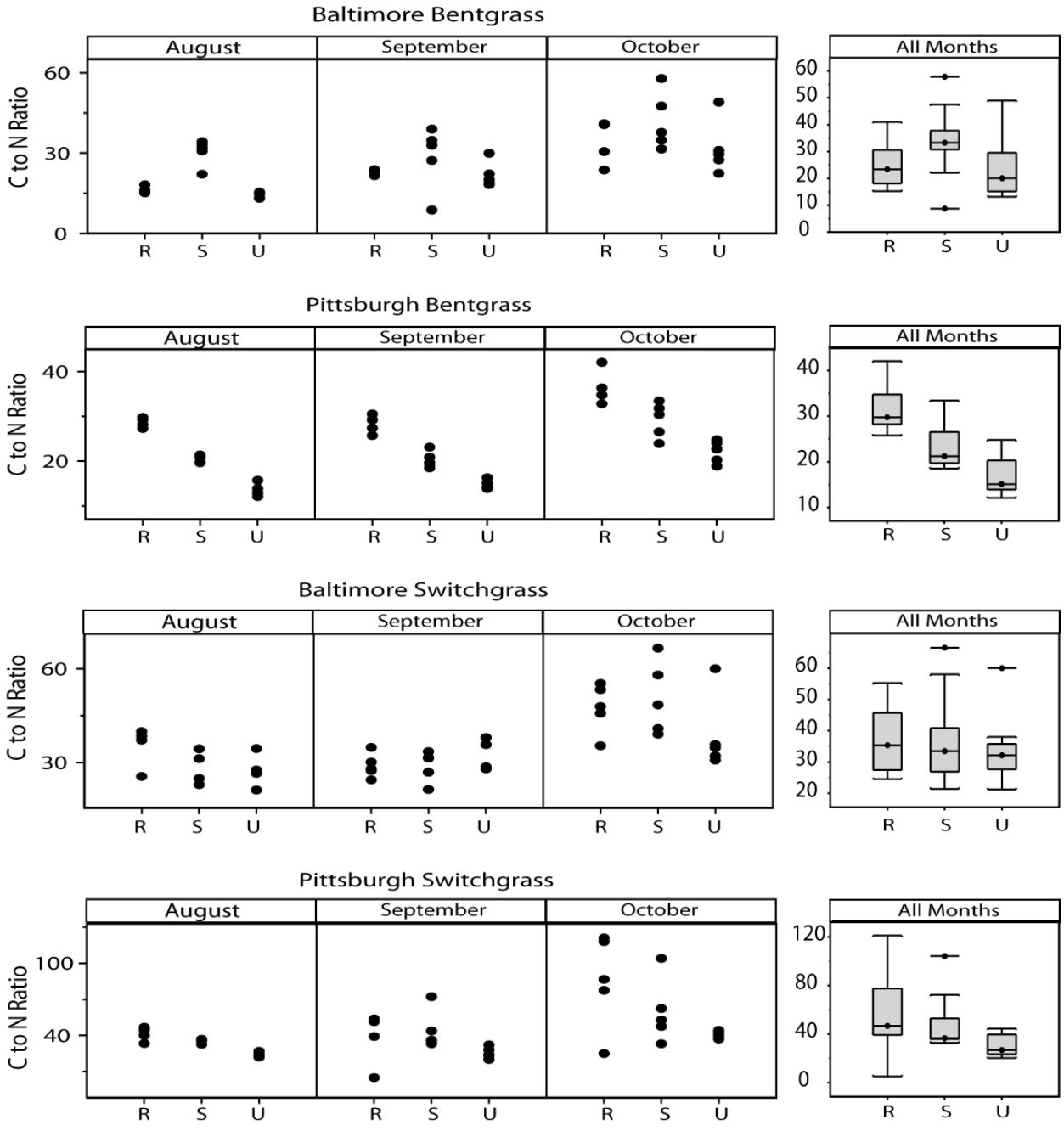

Figure 3.9 Plant tissue C to N molar ratios of Baltimore and Pittsburgh Bentgrass and Switchgrass.

Baltimore Switchgrass had similar values along the gradient, with no significant differences between sites (ANOVA, p=0.05) (Figure 3.9). The Pittsburgh Switchgrass showed a more pronounced gradient in C:N values. Urban sites had the lowest values, while rural sites had

the highest. The urban and rural site were significantly different (ANOVA, p=0.05). Like Bentgrass, Switchgrass at both gradients showed a distinct seasonal pattern, with lower values in August and September and higher values in October.

3.4 DISCUSSION

3.4.1 N fluxes and isotopes

Average total N fluxes (HNO_3 + NO_2) along the Baltimore and Pittsburgh gradients showed increased levels of N deposition in urban sites compared to rural sites (Figure 3.3a and b). This was expected due to increased fossil fuel sources in urban areas, particularly from mobile sources. N flux at the urban site was 1.5 times higher than at the rural site along the Baltimore gradient, and 2.3 times higher at the Pittsburgh site. Most national N monitoring network (e.g., CASTNET) sites are located in rural areas, thereby avoiding urban N deposition "hotspots". Furthermore, a large component of the N flux measured in this study was from NO_2, which is not measured by these networks. As a consequence, the results presented in this study indicate that national monitoring networks underestimate total dry N deposition reaching the landscape and further that spatial patterns of deposition should be accounted for in watershed N loading models.

While total N flux is on average greater at urban sites, monthly variation in HNO_3 and NO_2 flux reveals more complex deposition patterns (Figure 3.3c and d). For example, NO_2 flux increases in October and November at both gradients, corresponding with the winter changeover to non-reformulated gasoline, which does not burn as cleanly as summertime reformulated gas;

increased winter fossil fuel demand for heating and changes in atmospheric photochemistry in winter months. However, HNO_3 does not follow this pattern; highest HNO_3 flux along the Baltimore gradient was in September and along the Pittsburgh gradient was in July. In addition, relative contributions of HNO_3 and NO_2 differed by site, with higher proportions of HNO_3 deposition occurring at rural sites. This may be attributed to competing HNO_3 formation pathways, seasonal variation in stationary and mobile source emissions, and weather patterns (i.e. temperature, relative humidity and wind directions).

In order to better understand these complex trends in regional N flux, we can use $\delta^{15}N$ of dry deposition to help determine the sources of HNO_3 and NO_2 dry deposition (Figures 3.4 and 3.5). For example, $\delta^{15}N\text{-}NO_2$ along the Pittsburgh gradient was 5 to 20‰ higher at the urban site than at the rural site in every month. In contrast, $\delta^{15}N\text{-}NO_2$ at the Baltimore urban site was only higher in October and November. The higher $\delta^{15}N\text{-}NO_2$ suggests an influence of stationary source and vehicular NO_x at the urban sites, which is expected in urban areas. Pittsburgh may experience higher values at the urban site in all months of the study because it is downwind of the Ohio River Valley, which has the highest concentration of coal-burning power plants in the U.S.; thus it is likely that the Pittsburgh urban site is more heavily influenced by anthropogenic emissions than the Baltimore urban site.

Monthly $\delta^{15}N\text{-}NO_2$ data show temporal variations, with increased values in October and November at all sites along both gradients. Seasonal patterns in $\delta^{15}N\text{-}NO_2$ are consistent with other studies that report the $\delta^{15}N$ of dry N deposition in HNO_3 and particulate NO_3- [*Elliott et al.*, 2009] and NO_2 [*Freyer et al.*, 1993] where values are higher in the winter and lower in the summer. These patterns are attributed to changing NO_x oxidation pathways between summer and winter [*Freyer et al.*, 1993] and changes in stationary source NO_x emissions relative to

lightning and biogenic emissions in summer [*Elliott et al.*, 2009]. In this study, both mechanisms are likely for causing the seasonal variation in $\delta^{15}N\text{-}NO_2$. With the exception of the Pittsburgh urban site, which had values between -12 and -5‰ for every month, all sites had $\delta^{15}N\text{-}NO_2$ values between -26 and -22‰ in the summer months (July-September). In October and November, these values shifted upward by as much as 11‰ to a range of about -5 to -15‰. At these sites, $\delta^{15}N\text{-}NO_2$ values were reflective of biogenic NO_x emissions in the summer, during the growing season, and reflective of increasing proportional contributions from fossil fuel emissions during October and November.

Isotopic analysis of HNO_3 and NO_2 reveals that in this study, the sources of these two species may be different. For example, we can calculate the approximate $\delta^{15}N$ signature of the NO_2 from which HNO_3 originated. The oxidation of NO_2 to HNO_3 can result in a fractionation of 0.9971, causing $\delta^{15}N\text{-}HNO_3$ values to be ~3‰ lower than $\delta^{15}N\text{-}NO_2$ [*Freyer*, 1991]. Therefore, in order to calculate $\delta^{15}N\text{-}NO_2$ we can simply add 3‰ to our $\delta^{15}N\text{-}HNO_3$ value. Accounting for this fractionation, calculated results indicate HNO_3 originates as NO_2 with $\delta^{15}N\text{-}NO_2$ values ranging from 1.8‰ to 5.8‰ for both gradients. These values fall within the isotopic range of fossil fuel combustion from automobiles (-7 to +9‰) [*Ammann et al.*, 1999; *Freyer*, 1978; *Heaton*, 1990; *Moore*, 1977] and power plant combustion (+6 to +20‰) [*Felix et al.*, submitted; *Heaton*, 1990].

In contrast, our actual NO_2 measurements showed a much larger range in values, ranging from -26.4‰ to -7.7‰ for the Baltimore gradient and -26.6‰ to -5.7‰ at the Pittsburgh sites. These values are closer to values for biogenic NO_x (-19 to -49‰) [*Li and Wang*, 2008] and indicate mixing between biogenic and fossil fuel NO_2 sources. Because HNO_3 can have an atmospheric lifetime of several days before being deposited, the discrepancy between HNO_3 and

NO_2 $\delta^{15}N$ values could indicate that the HNO_3 at these sites was subject to atmospheric transport and possibly formed further from our study sites. Furthermore, there was little evidence of a gradient in $\delta^{15}N$-HNO_3 values along both gradients. These results suggest that HNO_3 forms primarily from stationary sources and may be transported across a wide area, encompassing the entirety of each urban to rural gradient. This suggestion is further supported by seasonal variation in $\delta^{15}N$-HNO_3 values along the Pittsburgh gradient, where $\delta^{15}N$-HNO_3 values are highest in July and August, dip down in September, and are high again in October and November. This pattern may correspond with regional fossil fuel generation and consumption for air conditioning in the summer months and heating in October and November as has been documented in other studies [*Elliott et al.*, 2007; *Elliott et al.*, 2009]. In addition, all sampling sites across both gradients were located far enough from major roadways that they were not likely heavily influenced by locally deposited dry N from automobile emissions (See Chapter 2.0).

3.4.2 Plant response to gradients in N flux

This study was designed to control as many variables as possible with respect to plant isotopic composition. Plants were potted in the same type of potting soil to prevent influences of native soil. Plants were also started from seed in the same location prior to being deployed in the field, so seedlings would start out with similar isotopic composition. By using this design, we hoped to restrict plant nutrients to the potting soil and atmospheric deposition. However, despite a gradient of N flux and $\delta^{15}N$-NO_2 at the Baltimore and Pittsburgh sites, plant tissue $\delta^{15}N$ did not exhibit a strong gradient for either type of grass (Figure 3.6).

For example, δ^{15}N-Bentgrass varied between gradients. At the Baltimore gradient, the suburban site had the lowest values, while at the Pittsburgh gradient the suburban site had the highest values. While δ^{15}N-HNO_3 did not exhibit any gradient during the growing season, there was a strong gradient in δ^{15}N-NO_2 at the Pittsburgh sites during the growing season. Therefore, in Pittsburgh we would expect plants at the urban site to have higher δ^{15}N than plants at the rural site. However, patterns for δ^{15}N-Bentgrass at both gradients did not show a relationship with N flux, nor did they track either δ^{15}N-HNO_3 or δ^{15}N-NO_2.

In contrast, there was a slight gradient in δ^{15}N-Switchgrass at the Baltimore and Pittsburgh sites. δ^{15}N values were highest at the Baltimore urban site. However, again this was not correlated with δ^{15}N-NO_2 or δ^{15}N-HNO_3, both of which did not exhibit isotopic gradients during the growing season at the Baltimore site. At the Pittsburgh gradient, δ^{15}N-Switchgrass was highest at the urban and suburban sites. We expected the urban site to have the highest δ^{15}N, given the strong gradient in δ^{15}N-NO_2; however, the suburban site actually had the highest values. One confounding factor in this study is the influence of wet N deposition on the isotopic composition of plant tissue. Because plants were exposed to rain water for the duration of the growing season, they may have received nutrients from NO_3- in rainwater. Rain may have had variations δ^{15}N values along both gradients, and especially the Baltimore gradient due to the length of the gradient (209 kilometers). This potential exposure may have dampened any isotopic variation expected from the influence of dry deposition. For future studies, it is recommended to measure both wet and dry deposition to assess the influence of atmospheric N on plant tissue.

In this study, Switchgrass at both gradients had lower δ^{13}C values at the urban site than at the rural site (Figure 3.7), which suggests uptake of ^{13}C-depleted fossil fuel CO_2. This was

especially evident along the Pittsburgh gradient where the rural site had the highest $\delta^{13}C$-Switchgrass values, the urban site had the lowest and the suburban site was in between. (At the Baltimore site, the suburban and rural sites had comparable $\delta^{13}C$ values, indicating similar influence from fossil fuel CO_2 at each of these sites.) Pittsburgh $\delta^{13}C$-Bentgrass was also lower at the urban site and higher at the suburban and rural sites. In contrast, Baltimore $\delta^{13}C$-Bentgrass had very similar values for the urban and rural sites. Some of the highest $\delta^{13}C$ values were at the urban site, contrary to our hypothesis.

The differences in observed $\delta^{13}C$ compositions between Switchgrass and Bentgrass along these gradients may be attributed to photosynthetic pathway. Switchgrass uses the C4 photosynthetic pathway, while Bentgrass is a C3 plant. By nature of these photosynthetic pathways, C3 plants are known to have a higher discrimination against the heavier C isotope [*Farquhar et al.*, 1989]. For example, C3 plants have lower $\delta^{13}C$ values (-30 to -22‰) and C4 plants have a higher $\delta^{13}C$ values (-14 to -10‰) due to the higher discrimination in C3 plants. In addition, C3 plants generally have a larger range in carbon isotopic values than C4 plants (~8‰ vs. ~4‰) [*Farquhar et al.*, 1989]. Because C4 plants have a lower discrimination, they may be better indicators of changes in $\delta^{13}C$ in polluted areas, and this could explain why Switchgrass plants displayed a more robust $\delta^{13}C$ gradient than Bentgrass plants in this study.

The difference in discrimination of C isotopes between Bentgrass and Switchgrass may also have affected the $\delta^{13}C$ vs. $\delta^{15}N$ plots (Figure 3.8). These plots provide a novel way to visualize the isotopic differences in C and N for urban and rural sites for Switchgrass, but not for Bentgrass. The Switchgrass plots show a fairly distinct difference between urban and rural sites, with urban sites plotting towards the bottom right, with lower $\delta^{13}C$ and higher $\delta^{15}N$, and rural sites plotting closer to the top left, with higher $\delta^{13}C$ and lower $\delta^{15}N$. The Baltimore Bentgrass

plot, on the other hand, has the urban and rural sites in the same location on the plot. The Pittsburgh Bentgrass also has urban values that plot in the same region as the rural values; it is also affected by the unexpectedly low $\delta^{15}N$ values for the urban site.

Another measure used to assess the effects of the N flux gradient on vegetation was carbon to nitrogen ratios in plant tissue, which can indicate the relative amount of N taken up by the plant. We would expect that in rural areas with lower N deposition, plants would be more N-limited and therefore have higher C:N. Conversely, in urban areas with high N deposition, plants would not be as N-limited and would take up excess N, resulting in lower C:N (Figure 3.9). For Baltimore gradient Bentgrass, C:N at urban sites was not much different from rural sites, but both were lower than the suburban site. This may indicate that plants at the rural site were not N-limited, as expected. For Switchgrass, plants at the Baltimore gradient showed a similar trend to the Bentgrass, in which C:N at the urban site was only slightly lower than the rural site. In contrast, Bentgrass along the Pittsburgh gradient exhibited a strong C:N gradient, which was maintained in all months of the study. This suggests that the rural site was more N-limited than the urban site, which corresponded to N flux at these sites. Pittsburgh Switchgrass also had a gradient in C:N. Both types of grasses at both gradients exhibited seasonal variation, in which C:N ratios increased in October. This corresponds with the end of the growing season, during which time plants relocate N from the shoots to the roots, causing the shoots to have decreased N [*Dickson*, 1989].

3.4.3 Conclusions

This study demonstrates the use of passive samplers and plants as biomonitors, which provide a relatively inexpensive method to measure and monitor the effects of N deposition in urban areas. Measuring and delineating the sources of N deposition in urban areas is crucial to understanding N flux across the regional landscape, as urban areas are hotspots for N pollution. This study demonstrated that N flux is greatly increased in urban areas. N isotopes indicate that this is likely due to the influence of fossil fuel combustion from point and mobile sources in urban areas. However, there are few monitoring sites located in or near urban areas, as national monitoring networks such as the National Atmospheric Deposition Program- National Trends Network and CASTNET have sites intentionally located in rural areas, far from point sources of pollution. While this provides good estimates of regional background levels of N pollution, it does not take into account the high levels of N deposition that may be occurring close to urban areas. Further characterization of these hotspots of N pollution is needed to fully comprehend the impact of these spatial patterns in reactive nitrogen deposition to human and ecosystem health.

The ambiguity of some of the results in this study points out some of the problems with using the traditional urban, suburban and rural convention in studying nitrogen deposition and its effects on biogeochemistry. The delineation of urban, suburban and rural in this study was based on descriptive land use characteristics (such as type of neighborhood). Perhaps it would be better to attempt to quantify the urban to rural gradient with a discrete measurement, such as road or population density. For example, the Baltimore urban site was arguably “more urban” than the Pittsburgh urban site, due to its proximity to a heavily trafficked and populated downtown.

The Pittsburgh urban site, in contrast, was located in a neighborhood about four miles from downtown, which did not have nearly as much activity (and therefore exposure to area sources of N pollution) as the Baltimore site. Likewise, the Pittsburgh rural site was probably the "most rural" of all the sites, with its location near forested and agricultural areas. While the Baltimore rural site was in the NJ Pine Barrens, it was located downwind of a heavily suburbanized area. Further work on this project could include quantifying the "urban level" of the six sites and comparing the results along a six-site gradient, rather than by city.

APPENDIX A

DATA TABLES

Table A1: Road gradient nitrogen isotope data. Missing data points had insufficient sample mass for analysis.

Distance from the Road (m)	Month	$\delta^{15}N\text{-}HNO_3$ (‰)	$\delta^{15}N\text{-}NO_2$ (‰)
2	August	3.1	-5.1
2	September	-0.9	-3.3
2	October	3.1	5.3
2	November	2.4	7.3
12	August	3.0	-11.7
12	September	-0.9	-16.7
12	October	3.3	-8.8
12	November	1.7	0.5
30	July	1.0	-16.3
30	August	2.1	----
30	September	-1.1	-16.5
30	October	1.9	-6.2
30	November	1.9	0.1
90	July	5.7	-12.4
90	August	1.8	----
90	September	-1.1	-24.6
90	October	1.7	-14.5
90	November	2.1	-5.1
188	July	3.3	----
188	August	2.1	----
188	September	-0.8	-21.8
188	October	0.9	-12.5

188	November	1.9	-5.8
460	July	2.5	----
460	August	2.0	-16.2
460	September	-0.6	-24.6
460	October	2.5	-18.3
460	November	1.6	-11.9

Table A2: Road gradient nitrogen flux data. All nitrogen fluxes are in kg ha^{-1} yr^{-1}. Missing data points are due to sampling site vandalism.

Distance from Road (m)	Month	NO_2 Golden	NO_2 Roadman High	NO_2 Roadman Low	HNO_3 Golden	HNO_3 Roadman
2	August	0.85	1.60	0.70	0.14	0.06
2	September	1.09	2.05	0.89	0.11	0.06
2	October	3.46	6.49	2.83	0.18	0.07
2	November	3.44	6.45	2.81	0.26	0.10
12	August	0.83	1.56	0.68	0.34	0.14
12	September	0.70	1.31	0.57	0.13	0.06
12	October	1.69	3.18	1.39	0.20	0.08
12	November	2.39	4.48	1.95	0.22	0.08
30	July	0.85	1.59	0.69	0.11	0.06
30	August	----	----	----	0.09	0.03
30	September	0.88	1.66	0.72	0.08	0.04
30	October	1.38	2.59	1.13	0.13	0.05
30	November	1.42	2.66	1.16	0.42	0.15
90	July	0.80	1.50	0.66	0.11	0.06
90	August	0.06	0.12	0.05	0.09	0.03
90	September	0.51	0.96	0.42	0.09	0.04
90	October	0.75	1.41	0.61	0.43	0.17
90	November	1.31	2.45	1.07	0.26	0.09
188	July	0.03	0.06	0.03	0.12	0.07
188	August	0.00	0.00	0.00	0.09	0.03
188	September	0.43	0.80	0.35	0.08	0.04
188	October	0.77	1.44	0.63	0.56	0.22
188	November	1.27	2.37	1.04	0.42	0.16
460	July	0.00	0.00	0.00	0.19	0.10
460	August	0.29	0.54	0.23	0.06	0.02
460	September	0.42	0.78	0.34	0.07	0.03
460	October	0.86	1.62	0.71	0.18	0.07
460	November	0.77	1.44	0.63	0.17	0.06

Table A3: Road gradient Bentgrass nitrogen and carbon isotopes, C to N ratios and soil nitrogen isotopes

Distance from the Road (m)	Month	Grass Type	$\delta^{15}N$ (‰)	$\delta^{13}C$ (‰)	C:N	$\delta^{15}N$ Soil (‰)
30	July	Bentgrass	2.7	-30.2	16.2	-2.7
30	August	Bentgrass	2.8	-29.0	22.3	-2.0
30	September	Bentgrass	2.1	-28.5	22.2	-1.0
30	October	Bentgrass	1.3	-27.6	29.8	-8.1
91	July	Bentgrass	2.1	-30.6	12.4	-1.2
91	August	Bentgrass	0.6	-28.8	42.0	-1.4
91	September	Bentgrass	-0.4	-27.8	13.0	-1.3
91	October	Bentgrass	0.3	-29.2	35.7	-2.0
188	July	Bentgrass	3.6	-29.4	14.1	-1.5
188	August	Bentgrass	0.6	-28.8	25.9	-2.8
188	September	Bentgrass	0.3	-27.4	27.6	-2.0
188	October	Bentgrass	-0.3	-26.8	37.8	-1.1
460	July	Bentgrass	4.0	-30.2	17.4	-1.5
460	August	Bentgrass	0.0	-29.3	28.3	-2.0
460	September	Bentgrass	-0.6	-27.4	26.1	-2.6
460	October	Bentgrass	-0.7	-26.8	41.5	-2.4

Table A4: Road gradient Switchgrass nitrogen and carbon isotopes, C to N ratios and soil nitrogen isotopes

Distance from the Road (m)	Month	Grass Type	$\delta^{15}N$ (‰)	$\delta^{13}C$ (‰)	C:N	$\delta^{15}N$ Soil (‰)
12	August	Switchgrass	-1.7	-11.9	18.51	-1.7
12	September	Switchgrass	1.7	-13.3	23.80	-1.3
12	October	Switchgrass	1.2	-13.2	23.16	----
12 (2nd)	August	Switchgrass	-1.9	-13.8	21.43	-1.8
12 (2nd)	September	Switchgrass	-1.3	-12.8	19.78	-1.9
12 (2nd)	October	Switchgrass	2.9	-13.5	30.79	----
30	July	Switchgrass	2.1	-13.0	21.14	-0.3
30	August	Switchgrass	1.7	-13.0	39.86	-2.0
30	September	Switchgrass	-0.4	-12.6	26.62	-0.4
30	October	Switchgrass	1.3	-12.8	23.42	-0.8
90	July	Switchgrass	-0.1	-12.0	16.83	-2.4
90	August	Switchgrass	2.0	-11.4	18.22	-0.4
90	September	Switchgrass	1.6	-12.3	23.48	-0.7
90	October	Switchgrass	2.9	-12.5	30.13	-1.3
188	July	Switchgrass	3.4	-12.1	17.12	-0.6
188	August	Switchgrass	-0.2	-11.8	40.26	-1.0
188	September	Switchgrass	-0.1	-12.2	58.84	-1.5
188	October	Switchgrass	-1.1	-12.5	73.00	-1.7
460	July	Switchgrass	0.4	-12.2	17.95	-1.6
460	August	Switchgrass	-1.9	-12.0	39.42	-1.0
460	September	Switchgrass	-1.0	-12.6	50.83	-0.9
460	October	Switchgrass	-2.7	-12.8	125.41	-1.0

Table A5: Baltimore gradient nitrogen flux and isotopes. Missing data points are due to insufficient sample mass for analysis.

Location Description	Location	Month	NO_2 Flux (kg ha^{-1} yr^{-1})	HNO_3 Flux (kg ha^{-1} yr^{-1})	$\delta^{15}N$-HNO_3 (‰)	$\delta^{15}N$-NO_2 (‰)
Urban	Baltimore	July	0.46	0.56	0.3	-26.4
Urban	Baltimore	August	0.32	0.44	0.9	-25.0
Urban	Baltimore	September	0.36	0.43	1.2	-24.1
Urban	Baltimore	October	1.37	0.50	1.6	-11.3
Urban	Baltimore	November	1.71	0.16	2.1	-7.7
Suburban	Cub Hill	July	0.22	0.16	2.1	----
Suburban	Cub Hill	August	0.69	0.08	-0.4	-22.1
Suburban	Cub Hill	September	0.23	1.20	2.2	-24.0
Suburban	Cub Hill	October	0.88	0.44	2.1	-12.1
Suburban	Cub Hill	November	0.99	0.14	2.7	-13.0
Rural	Silas	July	0.26	0.68	1.5	-24.4
Rural	Silas	August	0.14	0.23	0.3	----
Rural	Silas	September	0.08	1.64	2.0	----
Rural	Silas	October	0.32	0.05	-5.9	-14.7
Rural	Silas	November	0.56	0.22	1.0	-12.0

Table A6: Pittsburgh gradient nitrogen flux and isotopes. Missing data points are due to insufficient sample mass for analysis.

Location Description	Location	Month	NO_2 Flux (kg ha^{-1} yr^{-1})	HNO_3 Flux (kg ha^{-1} yr^{-1})	$\delta^{15}N$-HNO_3 (‰)	$\delta^{15}N$-NO_2 (‰)
Urban	Hazelwood	July	0.37	1.54	2.1	-11.9
Urban	Hazelwood	August	0.68	0.10	1.5	-8.9
Urban	Hazelwood	September	1.49	0.08	0.2	-10.5
Urban	Hazelwood	October	1.15	0.45	2.3	-6.0
Urban	Hazelwood	November	2.38	0.26	2.0	-5.7
Suburban	Westmoreland	July	0.21	0.40	1.9	-26.6
Suburban	Westmoreland	August	0.29	0.09	0.7	-22.8
Suburban	Westmoreland	September	0.32	0.08	0.4	-24.5
Suburban	Westmoreland	October	0.39	0.38	1.4	-25.3
Suburban	Westmoreland	November	1.13	0.31	1.2	-15.2
Rural	Powdermill	July	0.25	0.53	2.8	-22.5
Rural	Powdermill	August	0.13	0.07	1.9	----
Rural	Powdermill	September	0.33	0.07	-1.2	-23.7
Rural	Powdermill	October	0.89	0.85	-0.1	-13.7
Rural	Powdermill	November	1.16	0.40	0.7	-9.1

Table A7: Baltimore gradient Bentgrass nitrogen and carbon isotopes and C to N ratios

Location Description	Location	Month	Grass Type	Plant Number	$\delta^{15}N$	$\delta^{13}C$	C:N
Urban	Baltimore	July	Bentgrass	3	-1.1	-30.5	11.03
Urban	Baltimore	July	Bentgrass	4	-0.8	-30.0	10.62
Urban	Baltimore	July	Bentgrass	5	-0.9	-31.0	9.79
Urban	Baltimore	August	Bentgrass	1	-0.6	-29.5	15.34
Urban	Baltimore	August	Bentgrass	2	0.1	-28.7	15.13
Urban	Baltimore	August	Bentgrass	3	0.3	-28.9	14.78
Urban	Baltimore	August	Bentgrass	4	-0.1	-28.6	13.38
Urban	Baltimore	August	Bentgrass	5	-0.7	-27.0	13.18
Urban	Baltimore	September	Bentgrass	1	-0.2	-31.0	18.90
Urban	Baltimore	September	Bentgrass	2	0.2	-30.5	22.23
Urban	Baltimore	September	Bentgrass	3	0.1	-30.8	20.06
Urban	Baltimore	September	Bentgrass	4	0.1	-30.5	18.30
Urban	Baltimore	September	Bentgrass	5	-1.2	-20.9	29.96
Urban	Baltimore	October	Bentgrass	1	1.0	-31.2	22.43
Urban	Baltimore	October	Bentgrass	2	-0.3	-30.9	29.54
Urban	Baltimore	October	Bentgrass	3	0.2	-30.2	31.01
Urban	Baltimore	October	Bentgrass	4	-0.3	-31.2	27.42
Urban	Baltimore	October	Bentgrass	5	-0.6	-16.0	49.01
Suburban	Cub Hill	July	Bentgrass	1	-2.1	-31.8	16.81
Suburban	Cub Hill	July	Bentgrass	2	-1.8	-31.1	22.64
Suburban	Cub Hill	July	Bentgrass	3	-1.0	-31.6	20.74
Suburban	Cub Hill	July	Bentgrass	4	-0.5	-31.5	19.77
Suburban	Cub Hill	July	Bentgrass	5	-0.5	-31.4	21.56
Suburban	Cub Hill	August	Bentgrass	1	-1.5	-30.3	22.06
Suburban	Cub Hill	August	Bentgrass	2	-1.2	-29.8	34.23
Suburban	Cub Hill	August	Bentgrass	3	-0.6	-29.4	33.32
Suburban	Cub Hill	August	Bentgrass	4	-0.2	-30.2	32.20
Suburban	Cub Hill	August	Bentgrass	5	-0.5	-30.3	30.73
Suburban	Cub Hill	September	Bentgrass	1	-0.2	-30.1	8.73
Suburban	Cub Hill	September	Bentgrass	2	-1.1	-29.3	34.69
Suburban	Cub Hill	September	Bentgrass	3	-0.7	-28.8	38.94
Suburban	Cub Hill	September	Bentgrass	4	-0.6	-29.7	32.90
Suburban	Cub Hill	September	Bentgrass	5	-0.5	-29.7	27.24
Suburban	Cub Hill	October	Bentgrass	1	-0.3	-29.9	31.56
Suburban	Cub Hill	October	Bentgrass	2	-1.2	-28.9	34.86

Suburban	Cub Hill	October	Bentgrass	3	-0.7	-29.1	57.86
Suburban	Cub Hill	October	Bentgrass	4	-0.6	-29.7	47.56
Suburban	Cub Hill	October	Bentgrass	5	-0.4	-30.2	37.76
Rural	Silas	August	Bentgrass	1	-0.8	-30.6	18.11
Rural	Silas	August	Bentgrass	2	-3.1	-30.5	15.21
Rural	Silas	August	Bentgrass	4	-0.7	-30.1	15.97
Rural	Silas	September	Bentgrass	1	-0.1	-30.5	23.83
Rural	Silas	September	Bentgrass	2	0.4	-30.6	21.58
Rural	Silas	September	Bentgrass	4	0.1	-30.4	23.07
Rural	Silas	October	Bentgrass	1	-0.4	-30.4	40.59
Rural	Silas	October	Bentgrass	2	0.2	-29.3	41.00
Rural	Silas	October	Bentgrass	3	6.3	-31.2	23.70
Rural	Silas	October	Bentgrass	4	0.0	-30.1	30.57

Table A8: Baltimore gradient Switchgrass nitrogen and carbon isotopes and C to N ratios

Location Description	Location	Month	Grass Type	Plant Number	$\delta^{15}N$	$\delta^{13}C$	C:N
Urban	Baltimore	July	Switchgrass	1	-0.7	-12.1	11.91
Urban	Baltimore	July	Switchgrass	2	-1.5	-12.2	12.41
Urban	Baltimore	July	Switchgrass	3	-2.7	-11.8	12.68
Urban	Baltimore	July	Switchgrass	4	-2.2	-11.5	11.27
Urban	Baltimore	July	Switchgrass	5	-0.2	-11.5	13.35
Urban	Baltimore	August	Switchgrass	1	0.9	-13.4	26.95
Urban	Baltimore	August	Switchgrass	2	5.5	-13.6	27.64
Urban	Baltimore	August	Switchgrass	3	0.3	-13.4	34.46
Urban	Baltimore	August	Switchgrass	4	-0.7	-13.7	26.54
Urban	Baltimore	August	Switchgrass	5	2.1	-13.7	21.26
Urban	Baltimore	September	Switchgrass	1	1.7	-13.5	38.00
Urban	Baltimore	September	Switchgrass	2	7.6	-13.6	27.98
Urban	Baltimore	September	Switchgrass	3	3.1	-13.6	35.73
Urban	Baltimore	September	Switchgrass	4	-1.1	-13.6	38.05
Urban	Baltimore	September	Switchgrass	5	7.5	-13.5	28.59
Urban	Baltimore	October	Switchgrass	1	1.6	-13.8	32.13
Urban	Baltimore	October	Switchgrass	2	10.1	-13.8	34.74
Urban	Baltimore	October	Switchgrass	3	9.4	-13.6	35.79
Urban	Baltimore	October	Switchgrass	4	-1.4	-13.5	60.02
Urban	Baltimore	October	Switchgrass	5	5.6	-13.5	30.78
Suburban	Cub Hill	July	Switchgrass	1	-2.7	-12.9	16.76
Suburban	Cub Hill	July	Switchgrass	2	-3.7	-13.0	18.71
Suburban	Cub Hill	July	Switchgrass	3	-3.1	-12.8	23.13
Suburban	Cub Hill	August	Switchgrass	1	-2.3	-13.2	34.39
Suburban	Cub Hill	August	Switchgrass	2	-1.7	-12.9	31.30
Suburban	Cub Hill	August	Switchgrass	3	-2.1	-12.8	22.96
Suburban	Cub Hill	August	Switchgrass	4	-1.9	-13.0	34.37
Suburban	Cub Hill	August	Switchgrass	5	-2.8	-12.9	24.89
Suburban	Cub Hill	September	Switchgrass	1	-1.4	-13.6	31.60
Suburban	Cub Hill	September	Switchgrass	2	-0.7	-13.3	33.47
Suburban	Cub Hill	September	Switchgrass	3	-2.1	-13.5	26.92
Suburban	Cub Hill	September	Switchgrass	4	-2.3	-13.6	31.40
Suburban	Cub Hill	September	Switchgrass	5	-1.2	-13.5	21.39
Suburban	Cub Hill	October	Switchgrass	1	-1.8	-13.4	39.08
Suburban	Cub Hill	October	Switchgrass	2	-2.1	-13.3	66.56

Suburban	Cub Hill	October	Switchgrass	3	-2.2	-13.2	48.43
Suburban	Cub Hill	October	Switchgrass	4	-1.7	-13.3	58.03
Suburban	Cub Hill	October	Switchgrass	5	-2.2	-13.3	40.86
Rural	Silas	July	Switchgrass	1	-1.0	-13.0	17.24
Rural	Silas	July	Switchgrass	2	0.4	-13.0	17.17
Rural	Silas	July	Switchgrass	3	0.2	-12.9	18.20
Rural	Silas	July	Switchgrass	4	0.4	-13.2	18.24
Rural	Silas	July	Switchgrass	5	1.7	-13.3	18.59
Rural	Silas	August	Switchgrass	1	-0.1	-13.1	39.89
Rural	Silas	August	Switchgrass	2	1.6	-13.1	37.16
Rural	Silas	August	Switchgrass	3	0.7	-13.0	38.45
Rural	Silas	August	Switchgrass	4	-0.2	-12.9	25.55
Rural	Silas	August	Switchgrass	5	2.9	-12.9	25.50
Rural	Silas	September	Switchgrass	1	0.4	-13.6	34.82
Rural	Silas	September	Switchgrass	2	0.7	-13.6	30.16
Rural	Silas	September	Switchgrass	3	0.2	-13.4	28.04
Rural	Silas	September	Switchgrass	4	3.6	-13.4	24.49
Rural	Silas	September	Switchgrass	5	0.7	-13.5	27.45
Rural	Silas	October	Switchgrass	1	-1.7	-13.5	53.33
Rural	Silas	October	Switchgrass	2	1.9	-13.4	45.71
Rural	Silas	October	Switchgrass	3	-1.1	-12.8	47.93
Rural	Silas	October	Switchgrass	4	-1.7	-13.3	55.26
Rural	Silas	October	Switchgrass	5	5.0	-13.1	35.36

Table A9: Pittsburgh gradient Bentgrass nitrogen and carbon isotopes and C to N ratios

Location Description	Location	Month	Grass Type	Plant Number	$\delta^{15}N$	$\delta^{13}C$	C:N
Urban	Hazelwood	July	Bentgrass	1	-4.0	-31.0	10.56
Urban	Hazelwood	July	Bentgrass	2	-3.7	-31.5	10.33
Urban	Hazelwood	July	Bentgrass	3	-3.2	-31.1	9.40
Urban	Hazelwood	July	Bentgrass	4	-3.7	-31.4	10.86
Urban	Hazelwood	July	Bentgrass	5	-0.7	-31.2	9.24
Urban	Hazelwood	August	Bentgrass	1	-1.6	-28.9	13.89
Urban	Hazelwood	August	Bentgrass	2	-2.1	-29.0	12.10
Urban	Hazelwood	August	Bentgrass	3	-1.8	-28.8	12.83
Urban	Hazelwood	August	Bentgrass	4	-1.8	-29.9	15.72
Urban	Hazelwood	August	Bentgrass	5	0.1	-28.5	12.99
Urban	Hazelwood	September	Bentgrass	1	-1.2	-28.6	13.93
Urban	Hazelwood	September	Bentgrass	2	-1.2	-28.4	14.16
Urban	Hazelwood	September	Bentgrass	3	-0.9	-29.1	15.10
Urban	Hazelwood	September	Bentgrass	4	-0.8	-27.9	16.30
Urban	Hazelwood	September	Bentgrass	5	-0.5	-28.4	14.23
Urban	Hazelwood	October	Bentgrass	1	-1.6	-28.8	20.28
Urban	Hazelwood	October	Bentgrass	2	-1.2	-28.0	18.87
Urban	Hazelwood	October	Bentgrass	3	-1.2	-27.6	24.76
Urban	Hazelwood	October	Bentgrass	4	-1.6	-29.5	24.09
Urban	Hazelwood	October	Bentgrass	5	-0.9	-28.2	22.71
Suburban	Westmoreland	July	Bentgrass	1	2.6	-29.1	16.07
Suburban	Westmoreland	July	Bentgrass	2	-0.5	-29.4	16.78
Suburban	Westmoreland	July	Bentgrass	3	1.8	-29.9	16.34
Suburban	Westmoreland	July	Bentgrass	4	2.0	-29.1	16.32
Suburban	Westmoreland	July	Bentgrass	5	-1.8	-29.3	10.97
Suburban	Westmoreland	August	Bentgrass	1	0.4	-28.6	21.38
Suburban	Westmoreland	August	Bentgrass	2	-0.4	-28.0	21.00
Suburban	Westmoreland	August	Bentgrass	3	0.3	-28.0	21.23
Suburban	Westmoreland	August	Bentgrass	4	-0.5	-27.7	19.63
Suburban	Westmoreland	August	Bentgrass	5	0.7	-28.2	19.76
Suburban	Westmoreland	September	Bentgrass	1	-0.7	-26.6	23.10
Suburban	Westmoreland	September	Bentgrass	2	-0.4	-26.9	19.30
Suburban	Westmoreland	September	Bentgrass	3	-0.1	-28.0	18.52
Suburban	Westmoreland	September	Bentgrass	4	0.4	-27.7	19.70
Suburban	Westmoreland	September	Bentgrass	5	-0.4	-26.9	20.91

Suburban	Westmoreland	October	Bentgrass	1	-1.0	-27.4	33.42
Suburban	Westmoreland	October	Bentgrass	2	-1.1	-27.5	31.80
Suburban	Westmoreland	October	Bentgrass	3	-0.8	-28.1	23.97
Suburban	Westmoreland	October	Bentgrass	4	-0.1	-27.6	26.56
Suburban	Westmoreland	October	Bentgrass	5	-0.9	-27.1	30.39
Rural	Powdermill	July	Bentgrass	1	1.1	-30.2	18.48
Rural	Powdermill	July	Bentgrass	2	0.5	-30.0	18.83
Rural	Powdermill	July	Bentgrass	3	-0.2	-29.4	16.28
Rural	Powdermill	July	Bentgrass	4	2.0	-30.0	19.84
Rural	Powdermill	July	Bentgrass	5	1.0	-29.3	19.04
Rural	Powdermill	August	Bentgrass	1	-0.3	-29.1	29.26
Rural	Powdermill	August	Bentgrass	2	-0.2	-28.4	28.21
Rural	Powdermill	August	Bentgrass	3	-0.8	-28.4	27.27
Rural	Powdermill	August	Bentgrass	4	-0.3	-28.5	29.81
Rural	Powdermill	August	Bentgrass	5	-0.8	-27.3	29.75
Rural	Powdermill	September	Bentgrass	1	-1.0	-27.7	30.55
Rural	Powdermill	September	Bentgrass	2	0.0	-28.4	25.75
Rural	Powdermill	September	Bentgrass	3	-0.9	-27.2	29.25
Rural	Powdermill	September	Bentgrass	4	-0.6	-27.7	27.40
Rural	Powdermill	September	Bentgrass	5	-0.6	-26.9	29.22
Rural	Powdermill	October	Bentgrass	1	-1.2	-28.4	42.04
Rural	Powdermill	October	Bentgrass	2	-1.2	-27.5	36.37
Rural	Powdermill	October	Bentgrass	3	-1.1	-27.7	34.76
Rural	Powdermill	October	Bentgrass	4	-0.6	-28.0	32.79
Rural	Powdermill	October	Bentgrass	5	-1.1	-26.2	36.35

Table A10: Pittsburgh gradient Switchgrass nitrogen and carbon isotopes and C to N ratios

Location Description	Location	Month	Grass Type	Plant Number	$\delta^{15}N$	$\delta^{13}C$	C:N
Urban	Hazelwood	July	Switchgrass	1	-3.5	-13.3	14.75
Urban	Hazelwood	July	Switchgrass	2	-3.3	-12.9	18.79
Urban	Hazelwood	July	Switchgrass	3	-2.4	-12.9	16.59
Urban	Hazelwood	July	Switchgrass	4	-5.0	-12.8	13.98
Urban	Hazelwood	July	Switchgrass	5	-2.7	-13.2	18.36
Urban	Hazelwood	August	Switchgrass	1	-1.2	-13.4	26.75
Urban	Hazelwood	August	Switchgrass	2	-0.6	-13.7	23.17
Urban	Hazelwood	August	Switchgrass	3	-0.5	-13.0	21.96
Urban	Hazelwood	August	Switchgrass	4	-0.4	-12.8	23.44
Urban	Hazelwood	August	Switchgrass	5	-1.1	-13.1	24.75
Urban	Hazelwood	September	Switchgrass	1	-1.1	-13.9	28.01
Urban	Hazelwood	September	Switchgrass	2	-0.5	-14.1	23.32
Urban	Hazelwood	September	Switchgrass	3	-1.7	-13.5	24.07
Urban	Hazelwood	September	Switchgrass	4	-1.1	-13.8	20.15
Urban	Hazelwood	September	Switchgrass	5	-1.4	-13.7	32.28
Urban	Hazelwood	October	Switchgrass	1	-2.1	-13.7	39.68
Urban	Hazelwood	October	Switchgrass	2	-0.9	-13.9	37.11
Urban	Hazelwood	October	Switchgrass	3	-2.0	-13.7	44.39
Urban	Hazelwood	October	Switchgrass	4	-1.7	-13.5	40.44
Urban	Hazelwood	October	Switchgrass	5	-1.9	-13.3	42.20
Suburban	Westmoreland	July	Switchgrass	1	-1.0	-12.3	24.13
Suburban	Westmoreland	July	Switchgrass	2	-1.6	-12.6	19.76
Suburban	Westmoreland	July	Switchgrass	3	-0.5	-12.5	20.93
Suburban	Westmoreland	July	Switchgrass	4	-1.2	-12.5	18.26
Suburban	Westmoreland	July	Switchgrass	5	-1.2	-12.7	21.57
Suburban	Westmoreland	August	Switchgrass	1	-0.8	-12.4	36.76
Suburban	Westmoreland	August	Switchgrass	2	-1.2	-12.6	35.98
Suburban	Westmoreland	August	Switchgrass	3	-0.7	-12.3	32.73
Suburban	Westmoreland	August	Switchgrass	4	-0.1	-12.8	36.54
Suburban	Westmoreland	August	Switchgrass	5	-0.1	-12.9	35.72
Suburban	Westmoreland	September	Switchgrass	1	-1.7	-12.9	72.23
Suburban	Westmoreland	September	Switchgrass	2	-0.6	-13.3	35.74
Suburban	Westmoreland	September	Switchgrass	3	-1.0	-13.1	36.20
Suburban	Westmoreland	September	Switchgrass	4	-0.7	-13.3	33.15
Suburban	Westmoreland	September	Switchgrass	5	0.0	-13.4	43.90

Suburban	Westmoreland	October	Switchgrass	1	-3.1	-12.8	33.14
Suburban	Westmoreland	October	Switchgrass	2	-1.2	-12.8	47.63
Suburban	Westmoreland	October	Switchgrass	3	-2.3	-12.7	62.34
Suburban	Westmoreland	October	Switchgrass	4	-2.8	-12.9	104.07
Suburban	Westmoreland	October	Switchgrass	5	-0.3	-13.2	52.77
Rural	Powdermill	July	Switchgrass	1	1.0	-12.0	21.71
Rural	Powdermill	July	Switchgrass	2	-0.6	-11.8	16.42
Rural	Powdermill	July	Switchgrass	3	0.6	-12.0	23.54
Rural	Powdermill	July	Switchgrass	4	-1.1	-11.9	21.02
Rural	Powdermill	July	Switchgrass	5	0.1	-11.6	20.72
Rural	Powdermill	August	Switchgrass	1	-0.8	-11.9	46.88
Rural	Powdermill	August	Switchgrass	2	0.3	-11.9	33.50
Rural	Powdermill	August	Switchgrass	3	-1.8	-12.1	44.62
Rural	Powdermill	August	Switchgrass	4	-1.1	-11.9	40.12
Rural	Powdermill	August	Switchgrass	5	-1.6	-12.2	46.48
Rural	Powdermill	September	Switchgrass	1	-2.7	-12.3	39.15
Rural	Powdermill	September	Switchgrass	2	-1.2	-12.3	53.93
Rural	Powdermill	September	Switchgrass	3	-2.2	-12.4	51.48
Rural	Powdermill	September	Switchgrass	4	-2.9	-12.4	5.03
Rural	Powdermill	September	Switchgrass	5	-1.6	-12.6	167.60
Rural	Powdermill	October	Switchgrass	1	-2.8	-12.6	77.50
Rural	Powdermill	October	Switchgrass	2	-1.3	-12.4	121.01
Rural	Powdermill	October	Switchgrass	3	-2.6	-12.5	117.91
Rural	Powdermill	October	Switchgrass	4	-4.1	-12.6	24.96
Rural	Powdermill	October	Switchgrass	5	-3.9	-12.5	86.68

BIBLIOGRAPHY

Aber, J., W. McDowell, K. Nadelhoffer, A. Magill, G. Berntson, M. Kamakea, S. McNulty, W. Currie, L. Rustad, and I. Fernandez (1998), Nitrogen Saturation in Temperate Forest Ecosystems, *BioScience*, *48*(11), 921-934.

Ammann, M., R. Siegwolf, F. Pichlmayer, M. Suter, M. Saurer, and C. Brunold (1999), Estimating the uptake of traffic-derived NO_2 from ^{15}N abundance in Norway spruce needles, *Oecologia*, *118*(2), 124-131.

Angold, P. G. (1997), "The impact of a road upon adjacent heathland vegetation: effects on plant species composition", *Journal of Applied Ecology*, *34*(2), 409-417.

Atkins, D. H. F., and D. S. Lee (1995), Spatial and temporal variation of rural nitrogen dioxide concentrations across the United Kingdom, *Atmospheric Environment*, *29*(2), 223-239.

Atkins, D. H. F., and D. S. Lee (1998), Spatial and temporal variation of rural nitrogen dioxide concentrations across the United Kingdom, *Atmospheric Environment*, *29*(2), 223-239.

Bernhardt-Römermann, M., M. Kirchner, T. Kudernatsch, G. Jakobi, and A. Fischer (2006), Changed vegetation composition in coniferous forests near to motorways in Southern Germany: The effects of traffic-born pollution, *Environmental Pollution*, *143*(3), 572-581.

Bignal, K. L., M. R. Ashmore, A. D. Headley, K. Stewart, and K. Weigert (2007), Ecological impacts of air pollution from road transport on local vegetation, *Applied Geochemistry*, *22*(6), 1265-1271.

Blasing, T. J., C. T. Broniak, and G. Marland (2005), The annual cycle of fossil-fuel carbon dioxide emissions in the United States, *Tellus B*, *57*(2), 107-115.

Bradley, M. J., and B. M. Jones (2002), Reducing Global NOx Emissions: Developing Advanced Energy and Transportation Technologies, *AMBIO: A Journal of the Human Environment*, *31*(2), 141-149.

Bush, S. E., D. E. Pataki, and J. R. Ehleringer (2007), Sources of variation in $\delta^{13}C$ of fossil fuel emissions in Salt Lake City, USA, *Applied Geochemistry*, *22*(4), 715-723.

Butler, T. J., G. E. Likens, F. M. Vermeylen, and B. J. B. Stunder (2005), The impact of changing nitrogen oxide emissions on wet and dry nitrogen deposition in the northeastern USA, *Atmospheric Environment*, *39*(27), 4851-4862.

Bytnerowicz, A., P. Miller, D. M. Olszyk, P. J. Dawson, and C. A. Fox (1987), Gaseous and particulate air pollution in the San Gabriel mountains of Southern California, *Atmospheric Environment (1967)*, *21*(8), 1805-1814.

Bytnerowicz, A., M. J. Sanz, M. J. Arbaugh, P. E. Padgett, D. P. Jones, and A. Davila (2005), Passive sampler for monitoring ambient nitric acid (HNO_3) and nitrous acid (HNO_2) concentrations, *Atmospheric Environment*, *39*(14), 2655-2660.

Cape, J. N., Y. S. Tang, N. van Dijk, L. Love, M. A. Sutton, and S. C. F. Palmer (2004), Concentrations of ammonia and nitrogen dioxide at roadside verges, and their contribution to nitrogen deposition, *Environmental Pollution*, *132*(3), 469-478.

Casciotti, K. L., D. M. Sigman, M. G. Hastings, J. K. Böhlke, and A. Hilkert (2002), Measurement of the Oxygen Isotopic Composition of Nitrate in Seawater and Freshwater Using the Denitrifier Method, *Analytical Chemistry*, *74*(19), 4905-4912.

Clark-Thorne, S. T., and C. J. Yapp (2003), Stable carbon isotope constraints on mixing and mass balance of CO_2 in an urban atmosphere: Dallas metropolitan area, Texas, USA, *Applied Geochemistry*, *18*(1), 75-95.

Clarke, J. F., E. S. Edgerton, and B. E. Martin (1997), Dry deposition calculations for the clean air status and trends network, *Atmospheric Environment*, *31*(21), 3667-3678.

Dickson, R., E. (1989), Carbon and nitrogen allocation in trees, *Ann. For. Sci.*, *46*(Supplement), 631s-647s.

Elliott, E. M., C. Kendall, S. D. Wankel, D. A. Burns, E. W. Boyer, K. Harlin, D. J. Bain, and T. J. Butler (2007), Nitrogen Isotopes as Indicators of NO_x Source Contributions to Atmospheric Nitrate Deposition Across the Midwestern and Northeastern United States, *Environmental Science & Technology*, *41*(22), 7661-7667.

Elliott, E. M., C. Kendall, E. W. Boyer, D. A. Burns, G. G. Lear, H. E. Golden, K. Harlin, A. Bytnerowicz, T. J. Butler, and R. Glatz (2009), Dual nitrate isotopes in dry deposition: Utility for partitioning NO_x source contributions to landscape nitrogen deposition, *J. Geophys. Res.*, *114*(G4), G04020.

Farquhar, G. D., J. R. Ehleringer, and K. T. Hubick (1989), Carbon Isotope Discrimination and Photosynthesis, *Annual Review of Plant Physiology and Plant Molecular Biology*, *40*(1), 503-537.

Felix, J. D., E. M. Elliott, and S. L. Shaw (submitted), Nitrogen stable isotopic composition of NO_x emissions from two coal-fired power plants, *Geophysical Research Letters*.

Fitter, A. H., and R. S. R. Fitter (2002), Rapid Changes in Flowering Time in British Plants, *Science*, *296*(5573), 1689-1691.

Fraser, M. P., and G. R. Cass (1998), Detection of Excess Ammonia Emissions from In-Use Vehicles and the Implications for Fine Particle Control, *Environmental Science & Technology*, *32*(8), 1053-1057.

Freyer, H. D. (1978), Seasonal trends of NH^{4+} and NO^{3-} nitrogen isotope composition in rain collected at Jülich, Germany, *Tellus*, *30*(1), 83-92.

Freyer, H. D. (1991), Seasonal variation of $^{15}N/^{14}N$ ratios in atmospheric nitrate species, *Tellus B*, *43*(1), 30-44.

Freyer, H. D., D. Kley, A. Volz-Thomas, and K. Kobel (1993), On the Interaction of Isotopic Exchange Processes With Photochemical Reactions in Atmospheric Oxides of Nitrogen, *J. Geophys. Res.*, *98*(D8), 14791-14796.

Galloway, J. N., W. H. Schlesinger, H. Levy, II, A. Michaels, and J. L. Schnoor (1995), Nitrogen fixation: Anthropogenic enhancement-environmental response, *Global Biogeochem. Cycles*, *9*(2), 235-252.

Galloway, J. N., J. D. Aber, J. W. Erisman, S. P. Seitzinger, R. W. Howarth, E. B. Cowling, and B. J. Cosby (2003), The Nitrogen Cascade, *BioScience*, *53*(4), 341-356.

Galloway, J. N., et al. (2004), Nitrogen Cycles: Past, Present, and Future, *Biogeochemistry*, *70*(2), 153-226.

Garten, C. T. J. (1993), Variation in foliar ^{15}N abundance and the availability of soil nitrogen on Walker Branch Watershed, *Ecology Journal*, *74*(7), 2098-2113.

Gebauer, G., and E. D. Schulze (1991), Carbon and nitrogen isotope ratios in different compartments of a healthy and a declining *Picea abies* forest in the Fichtelgebirge, NE Bavaria, *Oecologia*, *87*(2), 198-207.

George, K., L. H. Ziska, J. A. Bunce, and B. Quebedeaux (2007), Elevated atmospheric CO_2 concentration and temperature across an urban-rural transect, *Atmospheric Environment*, *41*(35), 7654-7665.

Gilbert, N. L., M. S. Goldberg, J. R. Brook, and M. Jerrett (2007), The influence of highway traffic on ambient nitrogen dioxide concentrations beyond the immediate vicinity of highways, *Atmospheric Environment*, *41*(12), 2670-2673.

Golden, H. E., E. W. Boyer, M. G. Brown, E. M. Elliott, and D. K. Lee (2008), Simple approaches for measuring dry atmospheric nitrogen deposition to watersheds, *Water Resour. Res.*, *44*, W00D02.

Hanson, P. J., K. Rott, G. E. Taylor Jr, C. A. Gunderson, S. E. lindberg, and B. M. Ross-Todd (1989), NO_2 deposition to elements representative of a forest landscape, *Atmospheric Environment (1967)*, *23*(8), 1783-1794.

Hargreaves, K. J., D. Fowler, R. L. Storeton-West, and J. H. Duyzer (1992), The exchange of nitric oxide, nitrogen dioxide and ozone between pasture and the atmosphere, *Environmental Pollution*, *75*(1), 53-59.

Hastings, M. G., D. M. Sigman, and F. Lipschultz (2003), Isotopic evidence for source changes of nitrate in rain at Bermuda, *J. Geophys. Res.*, *108*(D24), 4790.

Hastings, M. G., E. J. Steig, and D. M. Sigman (2004), Seasonal variations in N and O isotopes of nitrate in snow at Summit, Greenland: Implications for the study of nitrate in snow and ice cores, *J. Geophys. Res.*, *109*(D20), D20306.

Hauglustaine, D. A., C. Granier, G. P. Brasseur, and G. Mégie (1994), The importance of atmospheric chemistry in the calculation of radiative forcing on the climate system, *J. Geophys. Res.*, *99*(D1), 1173-1186.

Heaton, T. H. E. (1990), $^{15}N/^{14}N$ ratios of NO_x from vehicle engines and coal-fired power stations, *Tellus B*, *42*, 304-307.

Högberg, P. (1997), Tansley Review No. 95 ^{15}N natural abundance in soil-plant systems, *New Phytologist*, *137*(2), 179-203.

Howarth, R., et al. (1996), Regional nitrogen budgets and riverine N & P fluxes for the drainages to the North Atlantic Ocean: Natural and human influences, *Biogeochemistry*, *35*(1), 75-139.

Hutchinson, G. L., R. J. Millington, and D. B. Peters (1972), Atmospheric Ammonia: Absorption by Plant Leaves, *Science*, *175*(4023), 771-772.

Idso, C. D., S. B. Idso, and R. C. Balling (2001), An intensive two-week study of an urban CO_2 dome in Phoenix, Arizona, USA, *Atmospheric Environment*, *35*(6), 995-1000.

Jung, K., G. Gebauer, M. Gehre, D. Hofmann, L. Weißflog, and G. Schüürmann (1997), Anthropogenic impacts on natural nitrogen isotope variations in *Pinus sylvestris* stands in an industrially polluted area, *Environmental Pollution*, *97*(1-2), 175-181.

Keeling, C. D. (1979), The Suess effect: $^{13}Carbon$-$^{14}Carbon$ interrelations, *Environment International*, *2*(4-6), 229-300.

Keeling, C. D., R. B. Bacastow, A. F. Carter, S. C. Piper, T. P. Whorf, M. Heimann, W. G. Mook, and H. Roeloffzen (1989), A three-dimensional model of atmospheric CO_2 transport based on observed winds, 1, Analysis of observational data, *Aspects of Climate Variability in the Pacific and the Western Americas, Geophys. Monogr. Ser*, *55*.

Kendall, C., and J. McDonnell (Eds.) (1998), *Isotope Tracers in Catchment Hydrology*, Elsevier, New York, NY.

Kimball, B. A., J. R. Mauney, F. S. Nakayama, and S. B. Idso (1993), Effects of increasing atmospheric CO_2 on vegetation, *Plant Ecology*, *104-105*(1), 65-75.

Kirby, C., A. Greig, and T. Drye (1998), Temporal and Spatial Variations in Nitrogen Dioxide Concentrations Across an Urban Landscape: Cambridge, UK, *Environmental Monitoring and Assessment*, *52*(1), 65-82.

Kirchner, M., G. Jakobi, E. Feicht, M. Bernhardt, and A. Fischer (2005), Elevated NH3 and NO2 air concentrations and nitrogen deposition rates in the vicinity of a highway in Southern Bavaria, *Atmospheric Environment*, *39*(25), 4531-4542.

Knobeloch, L., B. Salna, A. Hogan, J. Postle, and H. Anderson (2000), Blue babies and nitrate-contaminated well water, *Environmental health perspectives*, *108*(7), 675-678.

Kondo, Y., et al. (2008), Formation and transport of oxidized reactive nitrogen, ozone, and secondary organic aerosol in Tokyo, *J. Geophys. Res.*, *113*(D21), D21310.

Koopmans, C., A. Tietema, and A. Boxman (1996), The fate of ^{15}N enriched throughfall in two coniferous forest stands at different nitrogen deposition levels, *Biogeochemistry*, *34*(1), 19-44.

Koren, H. S., and M. J. Utell (1997), Asthma and the environment, *Environmental health perspectives*, *105*(5), 534-537.

Li, D., and X. Wang (2008), Nitrogen isotopic signature of soil-released nitric oxide (NO) after fertilizer application, *Atmospheric Environment*, *42*(19), 4747-4754.

Lichtfouse, E., M. Lichtfouse, and A. Jaffrézic (2002), $\delta^{13}C$ Values of Grasses as a Novel Indicator of Pollution by Fossil-Fuel-Derived Greenhouse Gas CO_2 in Urban Areas, *Environmental Science & Technology*, *37*(1), 87-89.

Marino, B. D., and M. B. McElroy (1991), Isotopic composition of atmospheric CO_2 inferred from carbon in C4 plant cellulose, *Nature*, *349*(6305), 127-131.

Matson, P., K. A. Lohse, and S. J. Hall (2002), The Globalization of Nitrogen Deposition: Consequences for Terrestrial Ecosystems, *AMBIO: A Journal of the Human Environment*, *31*(2), 113-119.

Moomaw, W. R. (2002), Energy, Industry and Nitrogen: Strategies for Decreasing Reactive Nitrogen Emissions, *AMBIO: A Journal of the Human Environment*, *31*(2), 184-189.

Moore, H. (1977), The isotopic composition of ammonia, nitrogen dioxide and nitrate in the atmosphere, *Atmospheric Environment (1967)*, *11*(12), 1239-1243.

Morino, Y., Y. Kondo, N. Takegawa, Y. Miyazaki, K. Kita, Y. Komazaki, M. Fukuda, T. Miyakawa, N. Moteki, and D. R. Worsnop (2006), Partitioning of HNO_3 and particulate nitrate over Tokyo: Effect of vertical mixing, *J. Geophys. Res.*, *111*(D15), D15215.

Nadelhoffer, K. J., and B. Fry (1994), Nitrogen isotope studies in forest ecosystems, in *Stable Isotopes in Ecology and Environmental Science*, edited by K. Lajtha and R. Michener, p. 22, Blackwell Scientific Publications, Cambridge, Massachusetts.

Nasrallah, H. A., R. C. Balling Jr, S. Mohammed Madi, and L. Al-Ansari (2003), Temporal variations in atmospheric CO_2 concentrations in Kuwait City, Kuwait with comparisons to Phoenix, Arizona, USA, *Environmental Pollution*, *121*(2), 301-305.

Neuman, J. A., et al. (2006), Reactive nitrogen transport and photochemistry in urban plumes over the North Atlantic Ocean, *J. Geophys. Res.*, *111*(D23), D23S54.

Nixon, S. (1995), Coastal marine eutrophication: A definition, social causes, and future concerns, *Ophelia*, *41*, 199-219.

O'Leary, M. H. (1981), Carbon isotope fractionation in plants, *Phytochemistry*, *20*(4), 553-567.

Padgett, P. E., H. Cook, A. Bytnerowicz, and R. L. Heath (2009), Foliar loading and metabolic assimilation of dry deposited nitric acid air pollutants by trees, *Journal of Environmental Monitoring*, *11*(1), 75-84.

Pataki, D., D. R. Bowling, and J. R. Ehleringer (2003), Seasonal cycle of carbon dioxide and its isotopic composition in an urban atmosphere: Anthropogenic and biogenic effects, *J. Geophys. Res.*, *108*(D23), 4735.

Pataki, D., T. Xu, Y. Luo, and J. Ehleringer (2007), Inferring biogenic and anthropogenic carbon dioxide sources across an urban to rural gradient, *Oecologia*, *152*(2), 307-322.

Pearson, J., and G. R. Stewart (1993), The deposition of atmospheric ammonia and its effects on plants, *New Phytologist*, *125*(2), 283-305.

Pearson, J., D. M. Wells, K. J. Seller, A. Bennett, A. Soares, J. Woodall, and M. J. Ingrouille (2000), Traffic exposure increases natural ^{15}N and heavy metal concentrations in mosses, *New Phytologist*, *147*(2), 317-326.

Pennsylvania_Department_of_Transportation (2009), Traffic volume map of Westmoreland County, PA, edited.

Pepin, S., and C. Körner (2002), Web-FACE: a new canopy free-air CO_2 enrichment system for tall trees in mature forests, *Oecologia*, *133*(1), 1-9.

Port, G. R., and J. R. Thompson (1980), Outbreaks of Insect Herbivores on Plants Along Motorways in the United Kingdom, *Journal of Applied Ecology*, *17*(3), 649-656.

Rabalais, N. N. (2002), Nitrogen in Aquatic Ecosystems, *AMBIO: A Journal of the Human Environment*, *31*(2), 102-112.

Roadman, M. J., J. R. Scudlark, J. J. Meisinger, and W. J. Ullman (2003), Validation of Ogawa passive samplers for the determination of gaseous ammonia concentrations in agricultural settings, *Atmospheric Environment*, *37*(17), 2317-2325.

Roorda-Knape, M. C., N. A. H. Janssen, J. J. De Hartog, P. H. N. Van Vliet, H. Harssema, and B. Brunekreef (1998), Air pollution from traffic in city districts near major motorways, *Atmospheric Environment*, *32*(11), 1921-1930.

Rowland, A. J., M. C. Drew, and A. R. Wellburn (1987), Foliar Entry And Incorporation Of Atmospheric Nitrogen Dioxide Into Barley Plants Of Different Nitrogen Status, *New Phytologist*, *107*(2), 357-371.

Saurer, M., P. Cherubini, M. Ammann, B. De Cinti, and R. Siegwolf (2004), First detection of nitrogen from NO_x in tree rings: a $^{15}N/^{14}N$ study near a motorway, *Atmospheric Environment*, *38*(18), 2779-2787.

Sigman, D. M., K. L. Casciotti, M. Andreani, C. Barford, M. Galanter, and J. K. Böhlke (2001), A Bacterial Method for the Nitrogen Isotopic Analysis of Nitrate in Seawater and Freshwater, *Analytical Chemistry*, *73*(17), 4145-4153.

Singer, B. C., A. T. Hodgson, T. Hotchi, and J. J. Kim (2004), Passive measurement of nitrogen oxides to assess traffic-related pollutant exposure for the East Bay Children's Respiratory Health Study, *Atmospheric Environment*, *38*(3), 393-403.

Smith, B., M. Nitschke, L. Pilotto, R. Ruffin, D. Pisaniello, and K. Willson (2000), Health effects of daily indoor nitrogen dioxide exposure in people with asthma, *European Respiratory Journal*, *16*(5), 879-885.

Socolow, R. H. (1999), Nitrogen management and the future of food: Lessons from the management of energy and carbon, *Proceedings of the National Academy of Sciences of the United States of America*, *96*(11), 6001-6008.

Stewart, G., M. Aidar, C. Joly, and S. Schmidt (2002), Impact of point source pollution on nitrogen isotope signatures $\delta^{15}N$ of vegetation in SE Brazil, *Oecologia*, *131*(3), 468-472.

Stewart, G. R., S. Schmidt, L. Handley, M. H. Turnbull, P. D. Erskine, and C. A. Joly (1995), ^{15}N natural abundance of vascular rainforest epiphytes: implications for nitrogen source and acquisition, *Plant, Cell & Environment*, *18*(1), 85-90.

Sutton, M. A., U. Dragosits, Y. S. Tang, and D. Fowler (2000), Ammonia emissions from non-agricultural sources in the UK, *Atmospheric Environment*, *34*(6), 855-869.

Tang, Y. S., J. N. Cape, and M. A. Sutton (2001), Development and Types of Passive Samplers for Monitoring Atmospheric NO_2 and NH_3 Concentrations, *The Scientific World Journal*, *1*, 513-529.

Thoene, B., P. SchrÖDer, H. Papen, A. Egger, and H. Rennenberg (1991), Absorption of atmospheric NO_2 by spruce (*Picea abies* L. Karst.) trees, *New Phytologist*, *117*(4), 575-585.

Townsend, A. R., et al. (2003), Human health effects of a changing global nitrogen cycle, *Frontiers in Ecology and the Environment*, *1*(5), 240-246.

Trenberth, K. E., J. T. Houghton, and L. G. Meira Filho (1996), Climate Change 1995, The Science of Climate Change, in *Climate Change 1995, The Science of Climate Change*, edited by J. T. Houghton, L. G. Meira Filho, B. A. Callander, N. Harris, A. Kattenberg and K. Maskell, pp. 51-64, The Press Syndicate of the University of Cambridge, Cambridge, UK.

Turns, S. R. (1996), *An Introduction to Combustion Concepts and Applications*, McGraw-Hill, New York.

U.S._EPA_CASTNET (2008), Trends in Wet and Dry N deposition at LRL117 (Laurel Hill), edited.

Velasco, E., S. Pressley, E. Allwine, H. Westberg, and B. Lamb (2005), Measurements of CO_2 fluxes from the Mexico City urban landscape, *Atmospheric Environment*, *39*(38), 7433-7446.

Vitousek, P. M., J. D. Aber, R. W. Howarth, G. E. Likens, P. A. Matson, D. W. Schindler, W. H. Schlesinger, and D. G. Tilman (1997), Human Alteration Of The Global Nitrogen Cycle: Sources And Consequences, *Ecological Applications*, *7*(3), 737-750.

Wellburn, A. (1990), Tansley Review No. 24 Why are atmospheric oxides of nitrogen usually phytotoxic and not alternative fertilizers?, *New Phytologist*, *115*(3), 395-429.

Weyer, P. J., J. R. Cerhan, B. C. Kross, G. R. Hallberg, J. Kantamneni, G. Breuer, M. P. Jones, W. Zheng, and C. F. Lynch (2001), Municipal Drinking Water Nitrate Level and Cancer Risk in Older Women: The Iowa Women's Health Study, *Epidemiology*, *12*(3), 327-338.

Wittwer, S. H., and B. R. Strain (1985), Carbon dioxide levels in the biosphere: Effects on plant productivity, *Critical Reviews in Plant Sciences*, *2*(3), 171 - 198.

Wolfe, A. H., and J. A. Patz (2002), Reactive Nitrogen and Human Health:Acute and Long-term Implications, *AMBIO: A Journal of the Human Environment*, *31*(2), 120-125.

Yu, C. H., M. T. Morandi, and C. P. Weisel (2008), Passive dosimeters for nitrogen dioxide in personal/indoor air sampling: A review, *J Expos Sci Environ Epidemiol*, *18*(5), 441-451.

Ziska, L. H., J. A. Bunce, and E. W. Goins (2004), Characterization of an urban-rural CO_2 /temperature gradient and associated changes in initial plant productivity during secondary succession, *Oecologia*, *139*(3), 454-458.

Ziska, L. H., K. George, and D. A. Frenz (2007), Establishment and persistence of common ragweed (*Ambrosia artemisiifolia* L.) in disturbed soil as a function of an urban–rural macro-environment, *Global Change Biology*, *13*(1), 266-274.

Ziska, L. H., D. E. Gebhard, D. A. Frenz, S. Faulkner, B. D. Singer, and J. G. Straka (2003), Cities as harbingers of climate change: Common ragweed, urbanization, and public health, *The Journal of allergy and clinical immunology*, *111*(2), 290-295.